R2 Resource Consultants, Inc.
15250 NE 95th Street
Redmond, WA 98052-2518
Phone: (425) 556-1288
Fax: (425) 556-1290
e-mail: mail@R2usa.com

Technical Memorandum

Date: February 17, 2015 Project Number: 2037.01/MM101

To: Bob Aldrich, Snohomish County Surface Water Management

From: Paul DeVries, Ph.D., P.E.

Subject: Reach Scale Geomorphic Analysis of Hydraulic, Hydrologic, and Sediment Conditions in the Snohomish River Between SR 522 and Ebey Slough

CONTENTS

1. INTRODUCTION 3
2. METHODS 7
2.1 LONGITUDINAL PROFILES 7
2.2 HYDRAULIC MODELING 8
2.2.1 Spatial Extent and Constraints of Model 8
2.2.2 Geometric Data Processing 9
2.2.3 Model Finite Element Mesh Development 12
2.2.4 Land Surface Characterization 13
2.2.5 2D Model Set Up and Calibration 13
2.3 SEDIMENT TRANSPORT MODELING 24
2.3.1 Sediment Transport Simulation Flows 27
2.3.2 Long Term Sediment Trapping Efficiency Analysis 29
2.4 AERIAL PHOTOGRAPH INTERPRETATION 32
2.4.1 Historic Channel Planform Mapping 32
2.4.2 Gravel/Sand Bar Area Mapping 33
2.5 AVULSION POTENTIAL ASSESSMENT 33
2.5.1 Individual Avulsion Potential Factors 33
2.5.2 Joint Avulsion Vulnerability Factors 35

3. RESULTS 37
3.1 LONGITUDINAL PROFILES 37
3.2 CALIBRATED HYDRODYNAMIC MODEL OUTPUT 39
3.3 SEDIMENT TRANSPORT MODELING 41
3.4 CHANNEL MIGRATION PATTERNS 45
3.5 GRAVEL/SAND BAR STORAGE AREA TRENDS 48
3.6 AVULSION RISK 48
4. SYNOPSIS OF ANALYSIS RESULTS AND IDENTIFICATION OF CONCEPTUAL RESTORATION PROJECTS 50
4.1 SUMMARY OF LARGE SCALE VARIATION IN REACH GEOMORPHIC CHARACTERISTICS 50
4.2 POTENTIAL RESTORATION PROJECTS 52
4.2.1 Floodplain and Side Channel Connectivity Projects 53
4.2.2 Instream Habitat Complexity Projects 55
4.2.3 Projects Identified Through Other Forums 56
4.3 LEVEL OF CONFIDENCE IN ANALYSIS AND RESULTS 57
5. REFERENCES 59

APPENDICES

Appendix A Magnified Views of Boxed Areas Delineated in Figure 14 Showing Predicted Velocity Vectors at Higher Resolution
Appendix B Plates

1. INTRODUCTION

R2 Resource Consultants Inc., (R2) is assisting Snohomish County Surface Water Management (SWM) with reach scale geomorphic analyses that will be used to support assessment and prioritization of river and fish habitat restoration possibilities in the Snohomish River, with a focus between SR 522 and the inlet to Ebey Slough (Figure 1). The analyses are intended to facilitate identifying restoration projects that address restoration needs identified in the 2005 Snohomish Watershed Chinook Salmon Recovery Plan. The projects should be consistent and compatible with natural reach scale hydraulic and sediment transport processes so that they are effective in restoring and protecting salmon habitat while considering constraints of land use and infrastructure in the reach**.** R2 worked closely with SWM staff in the collection and analysis of data specific to the reach geomorphic assessment and directed at the following goals:

1. Identify reach scale patterns in flooding and channel morphology;
2. Evaluate hydraulic and sediment transport processes that will influence future condition and channel location in the reach;
3. Identify the most geomorphically active and inactive segments in the reach; and
4. Qualify likelihood of project success associated with different restoration activities for each level of geomorphic activity, including channel connectivity, floodplain connectivity, and instream habitat structures.

The conceptual framework for the analysis is that specific project types will have highest probability of success if they are matched to the dominant reach scale geomorphic processes that affect their function. For example, projects that provide habitat more commonly found under dynamic channel shifting conditions have highest probability of functioning properly when they are located where hydraulic and sediment transport processes strongly favor deposition of sediments. These segments tend to be most active geomorphically. Conversely, projects that provide instream habitat structure will function best when they are located in reaches that are in approximate equilibrium in terms of sediment transport and channel movement (i.e., most inactive geomorphically). Matching project type accordingly is a critical first step towards implementation. In addition, the results of this assessment can be used to help stakeholders better understand river processes that may affect them and how the projects were identified to minimize the potential for unintended consequences.

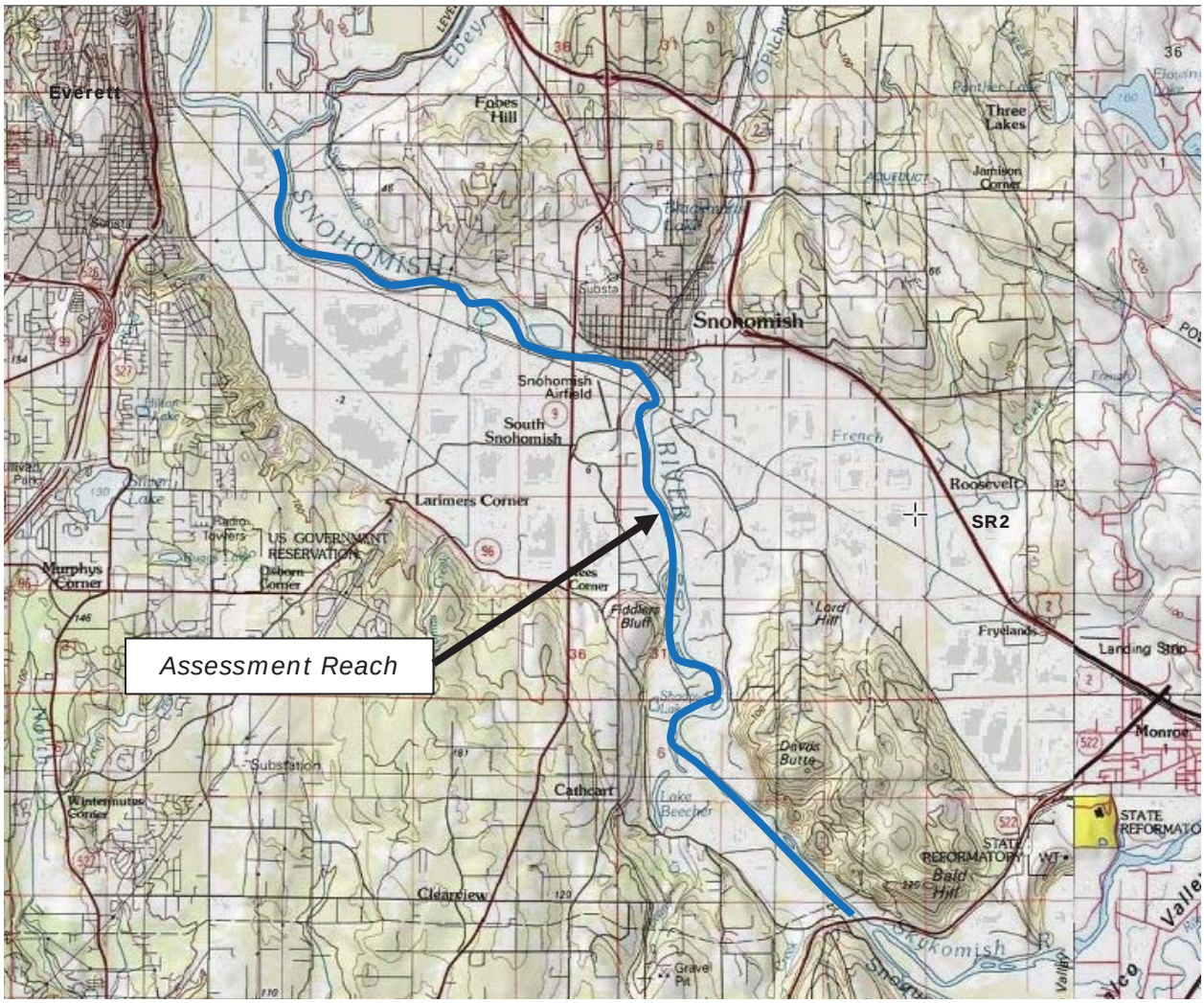

Figure 1. Location of the Snohomish River reach analyzed in this memorandum, between SR 522 and the head of Ebey Slough.

The geomorphic analysis involved the following elements that are described in this memorandum:

1. Collection and analysis of bed sediment sample and pebble count data, and analysis of long profile characteristics.
2. Development, calibration and use of a 2-dimensional (2D) hydrodynamic model in hydraulic and sediment transport analyses relative to identifying river segments with aggradational vs. degradation tendencies and for estimating hydraulic characteristics at various flow levels.

3. Digitizing of main and side channel locations and unvegetated gravel bars using available aerial photography up to and including 2012, and calculating channel migration rates.
4. Delineation of potential floodplain avulsion channels and assessment of avulsion risks.
5. Review and synthesis of the sediment transport, channel migration rate, and floodplain channel pathways data to develop ratings for each parameter for sub-reaches within the project reach (called analysis segments).
6. Identification of appropriate restoration project types for different segments based on segment characteristics developed in the preceding tasks.

This work is generally consistent with procedures used previously in the Sauk, Skykomish, Stillaguamish, and South Fork Stillaguamish rivers. The work products will be used to guide future restoration grant applications for completing projects that are consistent with natural geomorphic processes in the Snohomish River, and that have been determined in subsequent study and discussion to be compatible with land use and infrastructure constraints.

The analysis reach is about 12 miles long. The lower 9 miles of the reach experiences tidal fluctuations in river stage and has an extensive floodplain behind dikes that comprises important farmland. The reach provides important migration corridor and rearing habitat for Chinook salmon (*Oncorhynchus tshawytscha*), for which adult escapement numbers are estimated between 3%-6% of historic levels based on habitat capacity assessments as reported in the 2005 Snohomish Watershed Chinook Salmon Recovery Plan. More recent escapement data from 2005-2010 do not show any clear trends towards improvement of numbers (Snoqualmie Watershed Forum; *http://www.govlink.org/watersheds/7/status_report/Snoqualmie_Watershed_Status-Report_2005-2010.pdf*). As indicated in the plan, construction of levees, dikes, and other flood control structures and bank modifications, combined with draining and filling of side channels has significantly reduced the quantity and quality of salmonid rearing habitat and biological productivity in the assessment reach. Key objectives identified by the Recovery Plan for restoring habitat in the Snohomish River mainstem are to increase floodplain connectivity, channel complexity and provide juvenile rearing habitat along mainstem river margins in confined sections and off-channel floodplain habitats in unconfined sections. The analyses documented in this memo are key to understanding the reach scale processes that control the distribution, quality, and persistence of mainstem migration corridor and rearing habitat. Projects that are focused on enhancing migration and rearing habitat availability and quality are considered desirable for enabling recovery of Chinook salmon stocks in the basin.

The work and results described in this memorandum can be used to assess opportunities and risks of specific restoration activities designed to improve juvenile and spawning habitats, as well as more general risks to floodplain land use and infrastructure. To accomplish this, a strategy was employed of identifying the extent to which shorter, distinct segments within the reach are geomorphically active (or inactive) in terms of sediment transport, deposition, channel migration, and overall erosion tendency. This strategy allowed evaluation of the physical feasibility of specific project types and locations in the context of local and reach scale flooding and sedimentation process constraints.

This assessment is an important first step in planning for salmon recovery in the Snohomish River, where physical feasibility must be identified as explicitly as possible because the next, equally important step is to reconcile the resulting list of candidate projects with socio-economic and land use constraints. Much the Snohomish River floodplain has great economic importance for land use. The rationale for identifying a restoration project must be as clear as possible, and the results of the assessment facilitate explanation of the physical cause of specific effects to infrastructure and private land in an intuitive way to stakeholders. With this understanding, it is then possible to move forward with discussions of feasibility related to risks to infrastructure and land use.

2. METHODS

A suite of inter-related analyses was selected that facilitate identifying and locating site-specific restoration projects intended to increase instream and off-channel habitat quantity and quality for fish based on a sufficient understanding of reach-scale processes. Quantitative, process-based analyses (e.g., sediment transport modeling, bank migration rates, gravel bar areas) were favored over channel form (e.g., see Kondolf et al. 2001) or more complicated process-based classifications (e.g., channel migration zone mapping; Rapp and Abbe 2003). We followed the premise that for an assessment to lead directly to projects, it should involve identifying the feasibility of specific projects at selected sites subject to constraints posed by larger reach-scale natural processes. The analysis accordingly involved (1) identifying and quantifying physical processes that influence reach channel morphology, (2) modeling hydraulic and sediment transport processes that will affect future condition and channel location in the reach, and (3) using the results to identify the most geomorphically active and inactive segments in the reach. To accomplish these tasks, information was analyzed that was critical for assessing processes acting at the reach and site scales (Wissmar and Beschta 1998; Kondolf 2000): (1) longitudinal profiles of elevation, gradient, and grain size distributions, (2) hydraulics and hydrology using a 2D hydrodynamic model (RMA-2), USGS gage data, and surveyed cross-section and flood stage data, (3) bedload transport potential based on a 50-year duration, (4) aerial photographs for changes in active channel locations, and (5) LiDAR and other available GIS data for characterizing flood engagement frequency and avulsion risk potential of floodplain channels. Important details of the methods are described below.

2.1 Longitudinal Profiles

Longitudinal profiles provide an indication of effects of large scale slope changes on sediment transport and deposition patterns. Longitudinal profiles were developed for water surface and thalweg elevations over the analysis reach using the 2-D model data and predictions for the 2-yr flood event. The longitudinal profiles were plotted with grain size data to identify general sediment transport trends in the reach. A combination of sampling methods was used to characterize longitudinal variation in riverbed grain size, as described below.

Eleven grab samples were collected from the riverbed in the sand bed and the lower end of the gravel-sand transition zones on 12/16/03. Samples were collected with a Ponar sampler, which is a spring-activated bottom sampler best suited for silt, sand, and fine gravel substrates. The sampler was dropped to bottom and retrieved with a rope. The contents of the sampler were emptied into a plastic tub. Once a sufficient sample volume had been collected to meet general

sampling criteria of Church et al. (1987), the sediments were allowed to settle out, the overlying water poured off, and the remaining sediment-water mix was transferred to a 2-gallon Ziploc bag which was then double-bagged to prevent leakage and sample loss during transport. There was some ultrafine material suspended in the water poured off, but it accounted for a negligible fraction of the total sample weight.

The Ponar sampling results were combined with pebble count data collected previously at five locations upstream in the gravel bed zone as part of the Confluence Reach analysis (SWM 2003) to characterize overall upstream-downstream variation in grain size patterns in the reach. The pebble counts had been from active depositional point bars between the water and floodplain, at locations that were geomorphically similar in terms of bar type and relative location on the bar, so that observed longitudinal variation in grain sizes would not reflect locally variable depositional processes, but rather larger scale geomorphic variation. Various percentile particle sizes, including D_{50} (size for which 50 percent of stones were smaller), were computed for each sample and plotted against river mile.

2.2 Hydraulic Modeling

A 2D hydrodynamic unsteady flow model was constructed of the assessment reach river channel and floodplain using the SMS 10.0.11 modeling system, which integrates RMA2, a depth-averaged finite-element model supported by the Army Corps of Engineers (USACE) with a user-friendly interface for data pre- processing and post-processing. The model was used to predict water surface elevations and mean column velocities in the channel and over the floodplain, for analyzing off-channel habitat connectivity potential and sediment transport patterns in the main channel.

2.2.1 Spatial Extent and Constraints of Model

The river reach and floodplain area modeled (= “domain”) extends upstream from the inlet to Ebey Slough to the SR 522 bridge, below the confluence of the Snoqualmie and Skykomish rivers (Figure 2). The model domain spans the Snohomish River valley walls, including the floodplain area extending to the edge of the City of Monroe to the east and State Route SR-2 to the north-east. The Pilchuck River is the only significant tributary in the model area and enters the mainstem from the north near the City of Snohomish. The model domain extends partially up the Pilchuck River valley to approximately halfway between 92nd Street SE and 3 Lakes Road.

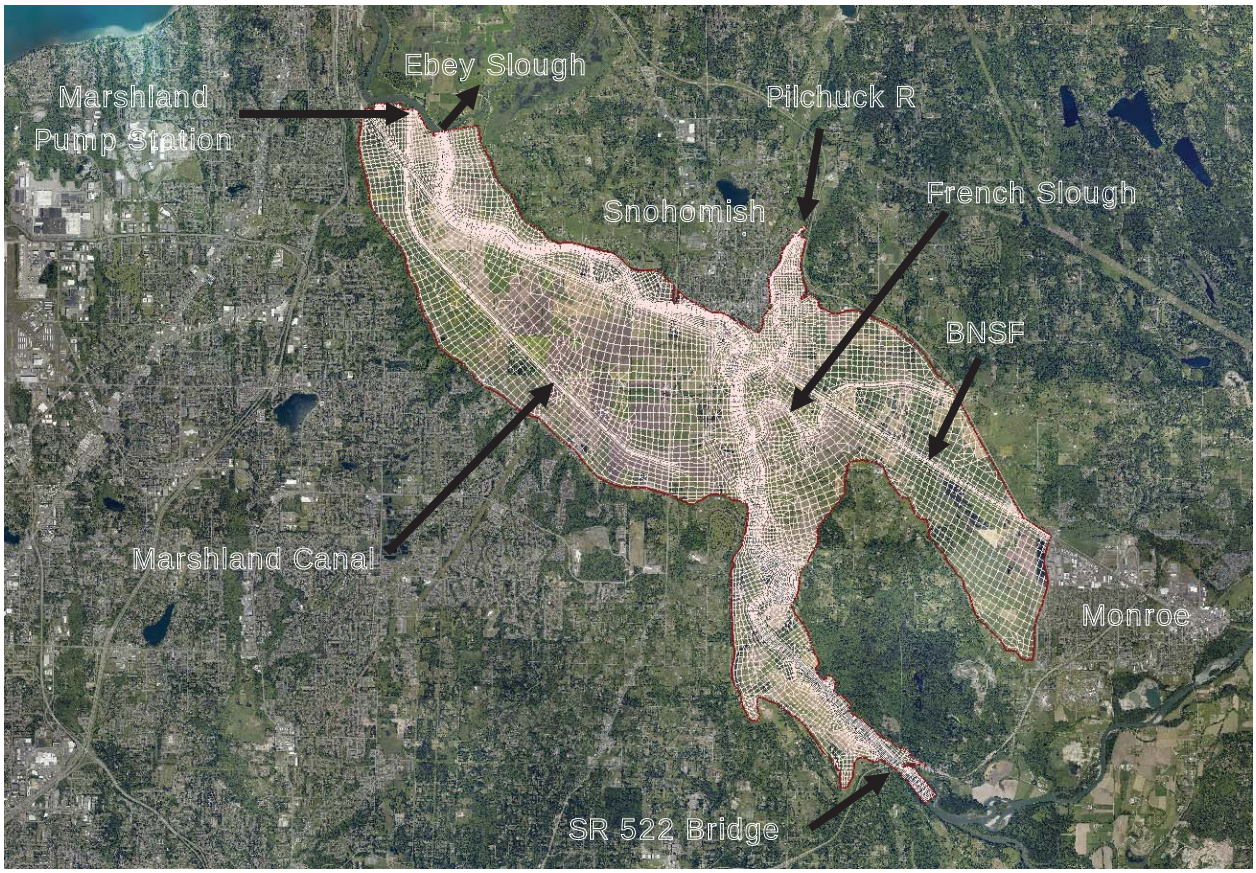

Figure 2. Geographic extent and resolution of the 2D hydrodynamic model domain and mesh analyzed in the assessment.

Flooding and floodplain flow patterns are strongly constricted in the assessment reach by roads, bridges, dikes, and railroad lines. Most of the left and right banks of the river are bounded by dikes that overtop during larger floods. The Burlington Northern Santa Fe (BNSF) railway embankment runs across the floodplain along the Lowell-Snohomish Road from the northwest corner of the modeling area toward the south-east of the modeling area to the City of Monroe. The railway divides the floodplain into two portions. The floodplain on the northeast side of the railway connects to the southwest side with four major bridge openings (the Marshland canal, Snohomish River, Pilchuck River, and French Slough) and several other smaller openings in the embankment.

2.2.2 Geometric Data Processing

The model topography was created using three sources of elevation data: LiDAR, a channel bathymetry survey, and a survey of levee/dike elevations. All data were provided by the County. The LiDAR elevation data had the greatest spatial resolution but lowest accuracy, whereas the

bathymetry and survey data were less extensive but had greater elevation accuracy. The bathymetry and ground survey data took precedence over the LiDAR data. The horizontal coordinate projection is NAD83 Washington State Plane North; the vertical datum is NAVD 88.

The LiDAR data were used to represent floodplain elevations, where flood water surface elevations and velocity gradients are generally mild. Data were provided initially in a 6 feet spatial grid, and subsequently filtered to a spatial resolution of 60 feet in each direction that was determined to be sufficient for simulating typical gradually varied flow patterns on the floodplain.

Greater emphasis for accuracy was placed on defining the topography of dikes, which influence the timing of overtopping and amount of overflow during a flood. All significant dikes in the assessment reach were mapped by County staff, with elevation points typically spaced 30-50 ft apart (Figure 3). The dikes were defined in the model as a denser line of interpolated points that mesh elements would not cross, with a spacing of 3 feet.

River channel bathymetry was mapped by the County in 2013 between the inlet to Ebey Slough and Thomas' Eddy using a combined RTK GPS and depth finder system. The bathymetry for the channel between Thomas' Eddy and the upstream boundary near SR-522 Bridge was imported from a 2-D model created of the Confluence Reach (SWM 2003).

In addition to several bridges crossing defined channels, there are multiple locations along the length of the BNSF railway grade that provide drainage across the grade divide. It was not possible to represent all of these to great detail in the model, thus their net hydraulic conveyance was modeled by creating ten openings distributed along the length of the grade. This allowed simulation of secondary drainage between the two sides of the floodplain bisected by the grade (with most drainage occurring through bridge openings). The hydraulics at all such openings were treated as open channel flow with control elevations based on ground survey data.

The model domain geometry was extended below Ebey Slough and above the SR 522 bridge, and the boundary ground elevations were lowered substantially. The model geometry was modified to rise gradually from the artificially lowered boundaries until it matched the actual topography. The purpose of this modification was to ensure that velocity distributions and directions and water depths predicted at the downstream and upstream limits of the assessment reach were not affected by numerical errors that can occur near model domain boundaries due to numerical errors. Specific modifications included:

- The upstream inflow boundaries of the Snohomish and Pilchuck rivers were extended upstream 2000 feet and 780 feet of the SR 522 and modified accordingly.
- The downstream outflow boundary required special treatment to allow the model to simulate the influence of tidal cycling. High tides cause a backwater and affect flow patterns in the channel, and depending on river flow, may be high enough for water to flow over the dike west of the Marshlands pump station. Also, as a numerical modeling feature, the initial starting water surface elevation (WSE) on the floodplain is set to be artificially higher than the dike and a mechanism is needed to drain the excess water. It was accordingly necessary to extend the mesh network west of the pump station and slide gates and extend it artificially outwards so that tide water could enter the floodplain and excess water on the floodplain could drain at the start of each simulation. During lower tides, there would be no water conveyed through this mesh except for a negligible pilot flow established specifically for numerical stability during the simulations.

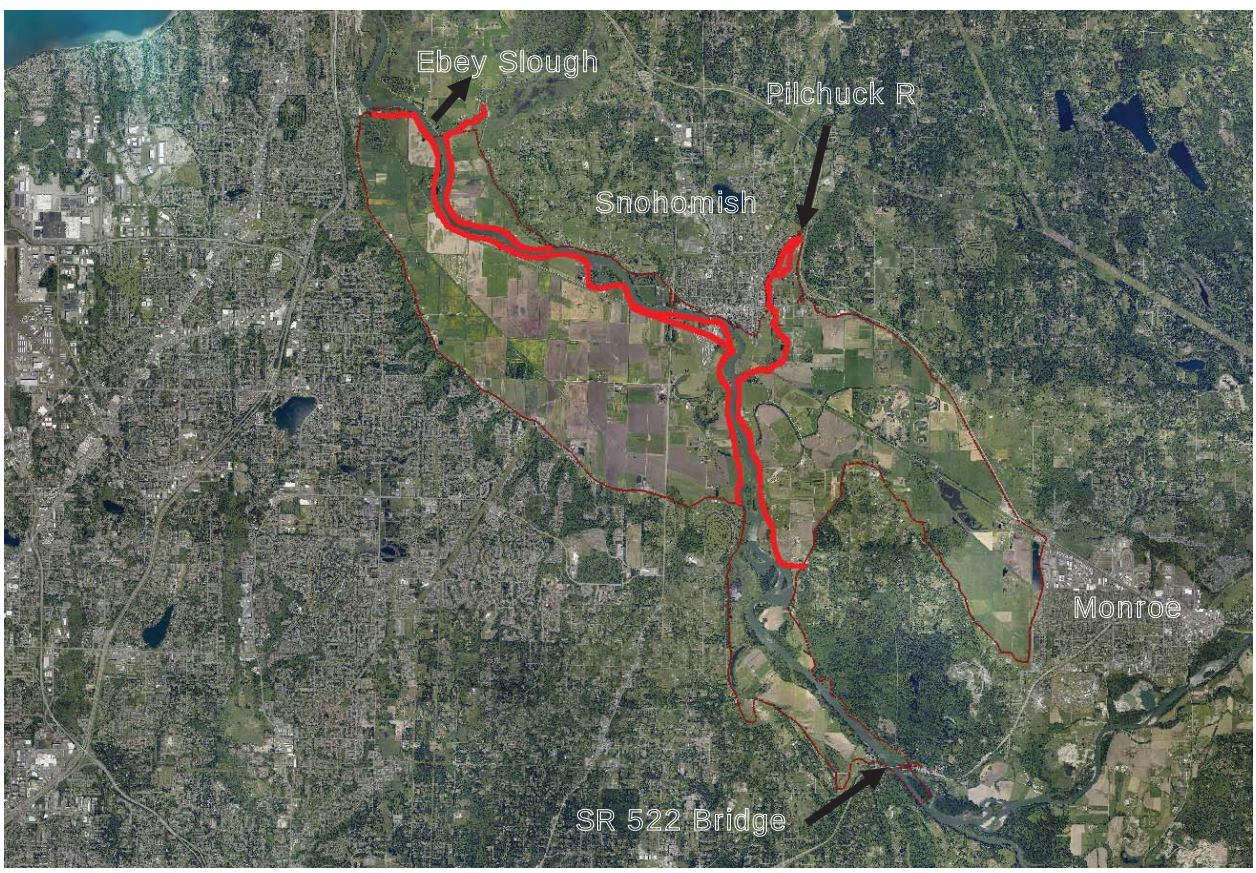

Figure 3. Segments of dikes where survey data were used to define their crest elevations in the 2D model.

In both cases, the sloping down of the ground to a lower elevation domain boundary was critical to meeting an RMA2 modeling requirement that inflow and outflow boundaries be wet at all times during a simulation.

2.2.3 Model Finite Element Mesh Development

The model mesh domain encompasses a representative topographic area of approximately 21.9 mi^2, plus 0.6 mi^2 for the extended boundary areas. A goal of mesh development was to minimize the number of elements to reduce model runtime to a reasonable duration. Given the large simulation area, mesh element sizes were designed strategically, using the combined topographic and bathymetric data to define mesh nodes. The resulting mesh consisted of both triangular elements with 6 nodes and quadrilateral elements with 8 nodes. The mesh elements were designed to be larger and the distance between nodes longer at locations where flood hydraulic properties were unlikely to change rapidly, such as on the floodplain. The elements were smaller and the distance between adjacent nodes shorter at locations where the terrain and/or hydraulics change rapidly in a short distance, such as in the vicinity of a dike and in the channel. In general, the element dimensions were on the order of 500 ft x 500 ft over most of the floodplain. Near hydraulic structures such as a dike or railroad grade, the element dimensions were on the order of 400 ft x 40 ft, with the longer side oriented parallel to the hydraulic structure. The resulting mesh network was made up of 37,552 nodal points in 13,617 elements, including 4,055 triangular and 9,562 quadrilateral elements (Figure 2). A triangular element was mainly used as a transition element to connect two quadrilateral elements.

The top widths of elevated topographic features such as dikes were on the order of ~10 to 20 ft, which presents special modeling issues. The RMA2 user's reference manual (King 2011) recommends the length to width ratio of an element not exceed 10, suggesting the longer side of an element should be only about 100 ft. Using such a small element would have required unreasonably long model run times to complete a simulation. To avoid this problem, the top widths of all elevated topographic features were increased artificially to about 40 ft, which would allow longer and thus fewer elements along the length of the linear feature. Even with this element size, the computer time for each model run was still just under two days on a 4th generation Intel i7 quad-core processor.

As a form of QA/QC check of the adequacy of the mesh to simulate the topographic effects of dikes and other structures, elevation contours were subsequently generated from the mesh network and compared with a contour map generated from the raw data. The comparison indicated the two contour maps were generally similar in the vicinity of hydraulic structures

where elevation changes were large over short distances. This confirmed that the meshing preserved the morphologic characteristics of the original basin topography during the triangulation and elevation interpolation process.

2.2.4 Land Surface Characterization

In additional to hydraulic conditions on the model boundary, the water movement within the model domain is also affected by the spatial variations in hydraulic roughness associated with different types of land cover on the floodplain. For example, densely forested areas slow down flow velocity compared with grass or crop cover.

Furthermore, as flows ascend and descend and tides rise and ebb, water levels fluctuate in response to those changes. Some areas may become dry as local WSE falls below the ground elevation and re-wet as WSE increases. To take into account the drying-wetting process, RMA2 provides a method called Marsh Porosity. This method numerically maintains a thin layer of water on the ground at all time to avoid a completely dry surface, and thus would enhance the model stability. The thickness of the water is between 0.0 ft and 0.2 ft during the modeling, with the actual depth dependent upon surrounding water surface elevation and ground elevation. The errors resulted from this thin layer of water should be acceptably insignificant for its negligible thickness.

A total of 35 types of land cover were used in the simulation, each with representative values of eddy viscosity, Manning's n roughness, and marsh porosity values (Figure 4; Table 1).

2.2.5 2D Model Set Up and Calibration

Before using the model for simulating proposed scenarios, it was necessary to ensure model accuracy by setting up boundary and initial conditions, and then calibrating and validating it to flood events with substantially different recurrence intervals. The 2D model was first calibrated to the January 2009 flood event, which represented around a 20 year recurrence interval at the upstream gage near SR 522. This event was selected because it had the most extensive post-flood survey data of high-water marks (HWMs) available compared with other recent floods within the project area. The model was then validated with the November 2008 event, which represented a 2-year recurrence interval.

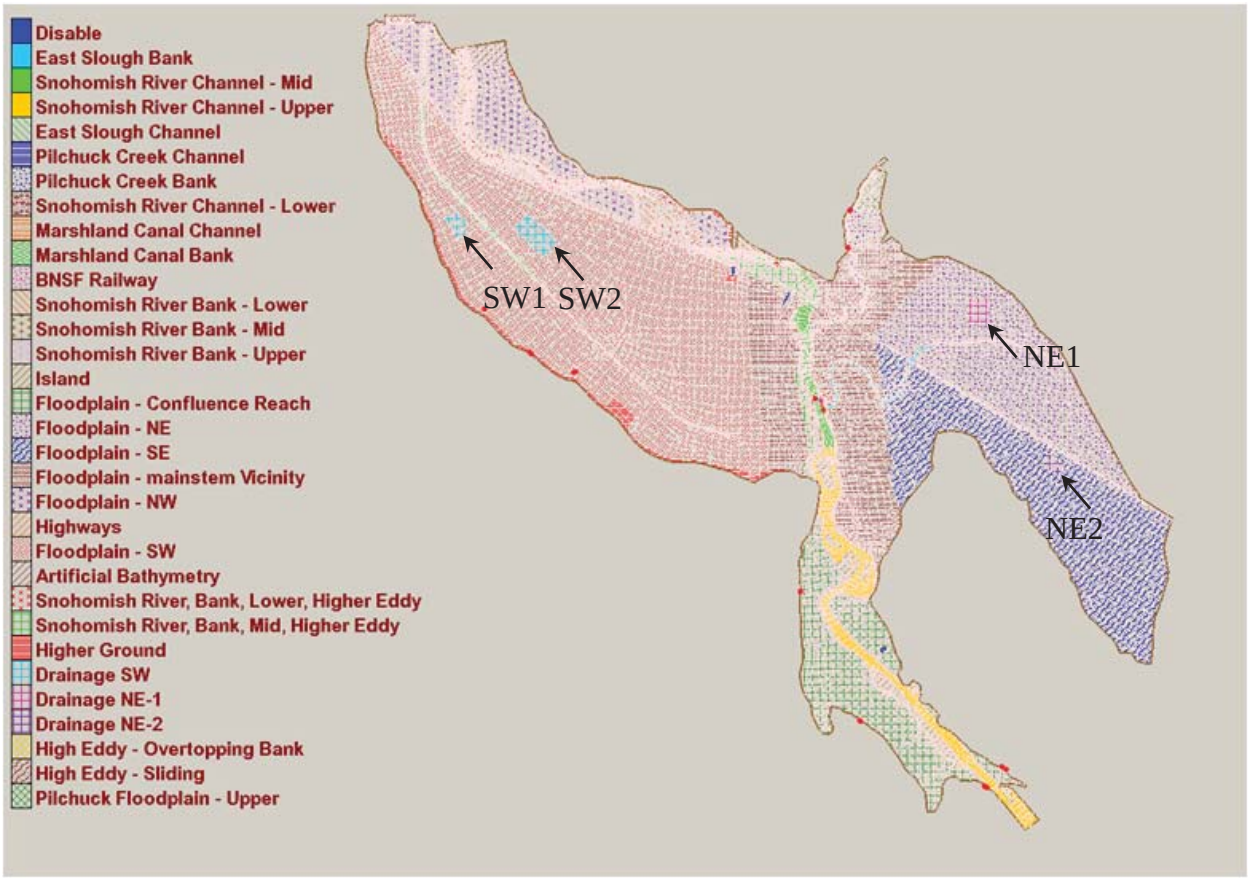

Figure 4. Material types used within the model domain designed to capture the hydraulic effects of different land covers. SW1, SW2, NE1, and NE2 are the four areas designated with element sinks described in Table 2.

2.2.5.1 Hydraulic Boundary Conditions

Boundary conditions are discharges and water surface elevations specified on the inflow and outflow portions of the model domain. The solution of a numerical simulation is the response of the model domain to the hydraulic conditions at the boundaries. For the current model, the Snohomish River flows entered from the southeast just upstream of SR-522 Bridge and the Pilchuck River flows from the north near the City of Snohomish. The downstream boundary was located just upstream of the Ebey Slough split where the water levels are strongly regulated by tides.

Table 1. Element Material Properties for Each Type of Land Cover Used in the Model Calibration to the January 2009 Flood Event.

	Land Use/ Element Material Type	Eddy Viscosity (lb-sec/ft^2)	Range of Manning 's n				Marsh Porosity		
			min	max	D1 (ft)	D2 (ft)	A1	A2	A3
1	East Slough Bank	60	0.05	0.08	1	0.01	40	2	0.004
2	Snohomish River Channel - Mid	50	0.038	0.046	2	0.1	25	2	0.002
3	Snohomish River Channel - Bank	60	0	0	0	0	35	2	0.004
4	Snohomish River Channel - Upper	50	0.032	0.038	2	0.1	25	2	0.002
5	East Slough Channel	50	0.035	0.055	0.5	0.01	35	2	0.003
6	Pilchuck Creek Channel	60	0.035	0.06	0.5	0.01	35	2	0.002
7	Pilchuck Creek Bank	60	0.05	0.08	1	0	35	2	0.002
8	Snohomish River Channel - Lower	50	0.03	0.035	2	0.1	25	2	0.002
9	Marshland Canal Channel	50	0.04	0.05	1	0.1	25	2	0.002
10	Marshland Canal Bank	60	0.05	0.07	1	0.1	35	2	0.004
11	BNSF Railway	60	0.06	0.09	0.2	0.1	40	2	0.003
12	Snohomish River Bank - Lower	80	0.06	0.09	0.5	0.01	35	2	0.002
13	Snohomish River Bank - Mid	70	0.1	0.2	1	0.1	35	2	0.002
14	Snohomish River Bank - Upper	60	0.06	0.08	1	0.1	35	2	0.002
15	Island	60	0.07	0.09	1	0	35	2	0.004
16	Floodplain - Confluence Reach	60	0.05	0.09	1	0	35	2	0.006
17	Floodplain - NE	50	0.05	0.07	1	0	35	2	0.003
18	Floodplain - SE	50	0.05	0.07	1	0	35	2	0.003
19	Floodplain - mainstem Vicinity	60	0.05	0.07	1	0	35	2	0.004
20	Floodplain - NW	50	0.05	0.08	1	0	35	2	0.003
21	Highways	80	0.05	0.07	0.5	0	40	2	0.003
22	Floodplain - SW	50	0.05	0.07	1	0	35	2	0.003
23	Artificial Bathymetry	250	0.03	0.05	1	0	35	2	0.004
24	Marshland Canal - High Eddy	160	0.06	0.09	0.5	0.1	35	2	0.005
25	Snohomish River, Bank, Lower, Higher Eddy	150	0.06	0.08	0.5	0	60	2	0.003
26	BNSF side	100	0.06	0.08	0.5	0.1	40	2	0.003
27	Snohomish River, Bank, Mid, Higher Eddy	150	0.07	0.09	0.5	0.02	40	2	0.004
28	Higher Ground	80	0.07	0.1	0.5	0.02	50	2	0.005
29	Drainage SW	50	0.05	0.07	0.5	0	35	2	0.004
30	Drainage NE-1	50	0.05	0.07	1	0	35	2	0.004
31	Drainage NE-2	50	0.05	0.07	1	0	35	2	0.004
32	High Eddy - Overtopping Bank	120	0.07	0.1	0.5	0.01	35	1	0.002
33	High Eddy - Sliding	200	0.06	0.08	0.5	0	35	2	0.005
34	Pilchuck Floodplain - Upper	90	0.06	0.09	0.5	0.01	35	2	0.004

Note: See RMA2 reference manual for the definitions of D1, D2, A1, A2, A3

The upstream boundary conditions were set as the flow hydrographs recorded at the USGS Gage #12150800 on the Snohomish River near Monroe, and at the USGS Gage #12155300 in the Pilchuck River near Snohomish. Flows from French Creek and small side tributaries to the river were considered negligible and were ignored.

The downstream boundary condition consisted of water surface elevation (WSE) time series. Predicted WSEs were provided by WEST Consultants (personal communication and email correspondence with R. Walton, March 10, 2014) for two flood events for use in model calibration and validation. The WSEs were predicted by a HEC-RAS model of the lower river that had been updated using the County's 2014 bathymetry data used in developing the 2D model; the data were shared collaboratively with WEST by R2 and the County. The WSE boundary conditions were applied to the outflow boundaries at Ebey Slough and near the Marshlands pump station.

Information was not available regarding how the Marshlands and French Creek pumps and gates were operated during the two simulated flood events. Assumptions were made about each that reflected ability to calibrate to surveyed high water marks on the floodplain. Knowledge of floodgate drain rates and pumping capacities would improve the calibration accuracy to reflect hydraulic conditions of each flood more specifically.

2.2.5.2 Spin-Down Boundary Conditions

When conducting simulations, it is easier for the RMA2 model to find a solution for 'mild' hydraulic conditions with low velocity and great flow depth. When depth is shallow and velocity fast, the model can have difficulty finding a convergent solution without appropriate initial conditions. Accordingly, the boundary conditions were set up specially to help the model reach a convergent solution, where the model domain was fully inundated with a large water depth at the beginning of the simulation, and the water level was then decreased ('spun down') gradually over a 10 hour period (model hours -18 to -8) at the downstream boundary to its level at the start of the actual flood hydrograph (model hour 0 = 11:00 pm on 1/6/09), with an intervening 8 hour period of steady inflow and WSE at the boundaries.

2.2.5.3 Establishing Initial Floodplain Conditions

To ensure the floodplain is adequately dry before floodwater starts to spill over stream banks, the element sink method available in RMA2 was used to emulate the effects of pump and floodgate to drain water off the floodplain. A sink involves a number of mesh elements situated at the lowest area of a region. This method removes a pre-determined time-dependent rate of water off

the floodplain through the elements designated for such draining. Using the water volume after the initial 10-hour spin down period and the total area of the elements designated for the drainage/sink, the drain rates were estimated for those elements to achieve a nearly dry condition on the floodplain before the flood arrived. A total of four areas were deployed with sink elements in the floodplain (Figure 4) with estimated drain rates listed in Table 2. The residual water depth on the floodplain prior to the arrival of flood generally ranged between 0.1 ft and 2 ft with an average value less than 0.3 ft. This residual depth should not be expected to have a significant impact on the predicted floodplain hydraulics or timing of peak flow.

Table 2. Element sink rate (cfs per square foot) of the 4 flow sinks defined in the 2D model calibration to the January 2009 flood event. The rates are designed to obtain a nearly dry condition in each region before flood water starts to spill over stream banks onto the floodplain and to emulate the floodgate/pump draining rates during the flood. DA = drainage area.

Hour	Element Drain Rate (cfs per unit square foot)			
	SW1 – near Valley Wall (DA = 0.04 mi^2)	SW2 – near BNSF (DA = 0.10 mi^2)	NE1 – North of BNSF(DA = 0.06 mi^2)	NE2 – South of BNSF (DA = 0.03 mi^2)
-18	0.01	0.01	0.015	0.025
-12	0.022	0.019	0.04	0.0184
-8	0.03	0.025	0.0333	0.014
-6	0.02	0.01	0.03	0.003
0	0.01	0.005	0.0171	0.00083
1	0.005	0.002	0.015	0.00046
2	0.0035	0.0015	0.005	0.0001
3	0.002	0.001	0.0025	0.00005
4	0	0	0	0
7	0	0	0	0
22	0	0	0	0
32	0.002	0.002	0	0
37	0.0025	0.0025	0	0
42	0.0035	0.003	0	0
52	0.0045	0.004	0	0
62	0.004	0.004	0	0
72	0.002	0.002	0	0
82	0.002	0.002	0	0
92	0.001	0.001	0	0
101	0.001	0.001	0	0

2.2.5.4 Simulation Time-Step and Duration

The simulation was conducted with a dynamic, time-dependent process. The solution for the current time t was used as the initial condition for the next time step $t+\Delta t$, with Δt being the time increment between two consecutive time steps. Typically between 1 and 4 iterations were needed to reach a convergent solution within a time step. Three time increments (0.1, 0.05, and 0.02 hr) were tested to determine the adequacy of time increment for modeling accuracy, stability and convergence. A comparison of the simulation results from the three time increments showed no significant differences in water depth or velocity at peak flow. To ensure a better convergence and to minimize the model run time, the time step Δt = 0.05 hour was selected for the model simulation.

At the beginning of a simulation (Model Hour -18), the initial condition consisted of zero velocities and water depths that equaled the difference between the assumed starting water surface elevation of 44.0 ft and the local ground elevation. The simulation was conducted for a total of 119 model hours including the first 18 hours of the 'spin-down' period, followed by 101 hours (1/6/2009 11 pm to 1/11/2009 4 am = model hours 0 to 101) of actual flow and stage hydrographs (Figure 5).

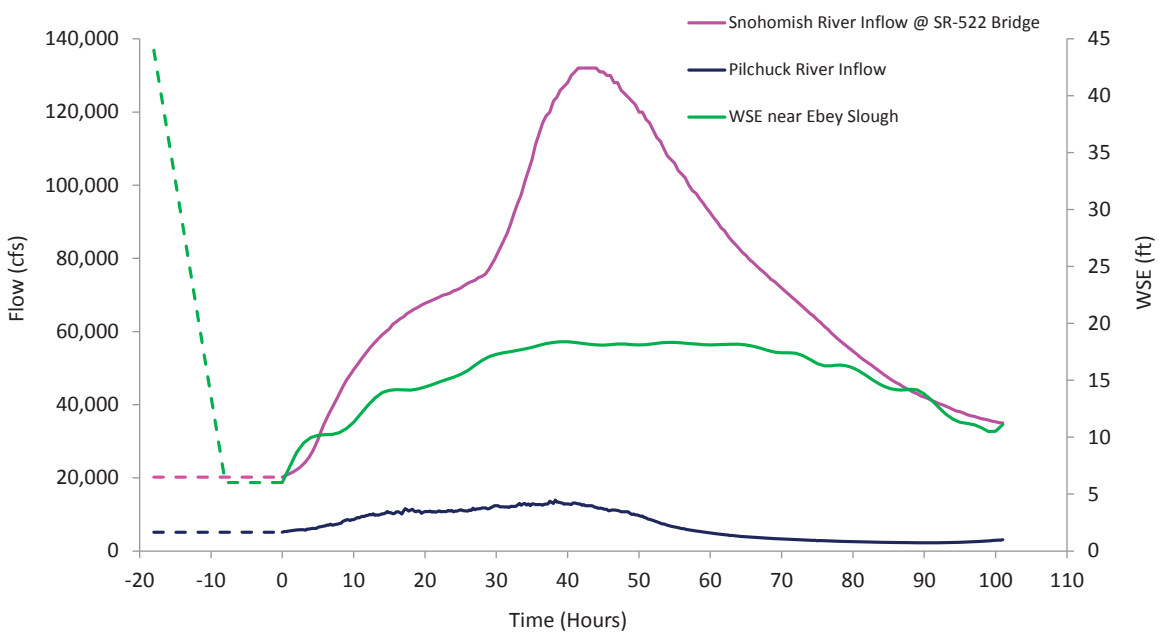

Figure 5. Hydrographs used in the hydraulic calibration. The time series in the first 18 hours (Hour -18 to Hour 0) are artificial to help the model establish a suitable initial condition at the time the actual hydrographs start on January 6, 2009 11 pm (Hour 0).

2.2.5.5 Model Calibration and Validation

Calibration

Calibration involved matching predicted water surface elevations with recorded values including surveyed HWMs and water surface elevation time series recorded at the County's French Creek Pump Station stage gage, and two USGS gages in the Snohomish River near Monroe (#12150800) and at Snohomish (#12155500). The large number of elements and complex system of hydraulic structures in the modeling area complicated the simulation and resulted in calibration requiring an extensive effort. In addition, calibration of floodplain water levels was difficult because of the lack of information on drainage and pumping rates, and of time varying WSEs during floods.

The process generally required iterative adjustments of element properties (see Table 1) such as Manning's n values, porosity, and eddy viscosity to satisfy all hydraulic conditions imposed on the model boundary for the entire simulation period. In addition, calibration involved iterative modifications to element sizes and orientations to achieve faster model convergence and better stability. Drainage rates specified for each of the four element sinks also required iterative adjustments to ensure the residual water on the floodplain prior to the arrival of flood wave did not substantially influence predicted floodplain hydraulics.

HWMs were surveyed at 16 locations (Figure 6; Table 3). Calibrated water levels were compared to the surveyed data. Predicted values for the Pilchuck River at the 2nd & 6th street bridges were found to not match the surveyed values as well as the other points in Table 3, which reflected primarily local bridge hydraulics and absence of accurate bathymetry data there. These points were thus not considered further in the calibration. The other water surface calibration errors, equal to the difference between surveyed HWMs and simulated peak WSE elevations, are summarized in Table 4. A positive difference means an over-prediction (i.e., simulated WSE is higher than HWM), and a negative means an under-prediction.

Figure 7 indicates there were several locations where HWMs were measured in close proximity. The surveyed elevations listed in Table 3 indicated some proximal HWMs were not consistent. For example, the two HWMs at the SR-522 Bridge had a 1.67 ft difference with downstream HWM higher than the upstream one. In hydraulic calibration, instead of trying to match with each individual HWM, it was decided to calibrate to the average elevation of the proximal HWMs. Table 4 summarizes the errors of the calibrated WSE resulting from such calibration strategy. At this modeling scale, FEMA guidelines are that model predictions of peak stage should match measured within ±0.5 ft. Of the 7 calibration errors listed in Table 4, there are four

(4) calibration errors less than 0.5 ft, one (1) less than 1 ft, and two (2) less than 2 ft. An error more than a foot suggests the adequacy of one or multiple data sources (e.g., boundary conditions, surveyed HWM elevations, basin topographic data, and etc.) used may be in question.

In addition to errors associated with incomplete information on pumping and flood gate operations, another source of calibration error appeared to be associated with errors in field identification of HWM elevations. The HWMs were not surveyed at the time flow peaked, and thus there were likely errors in interpretation based on washlines and debris signs that can be affected by wave actions and local terrain.

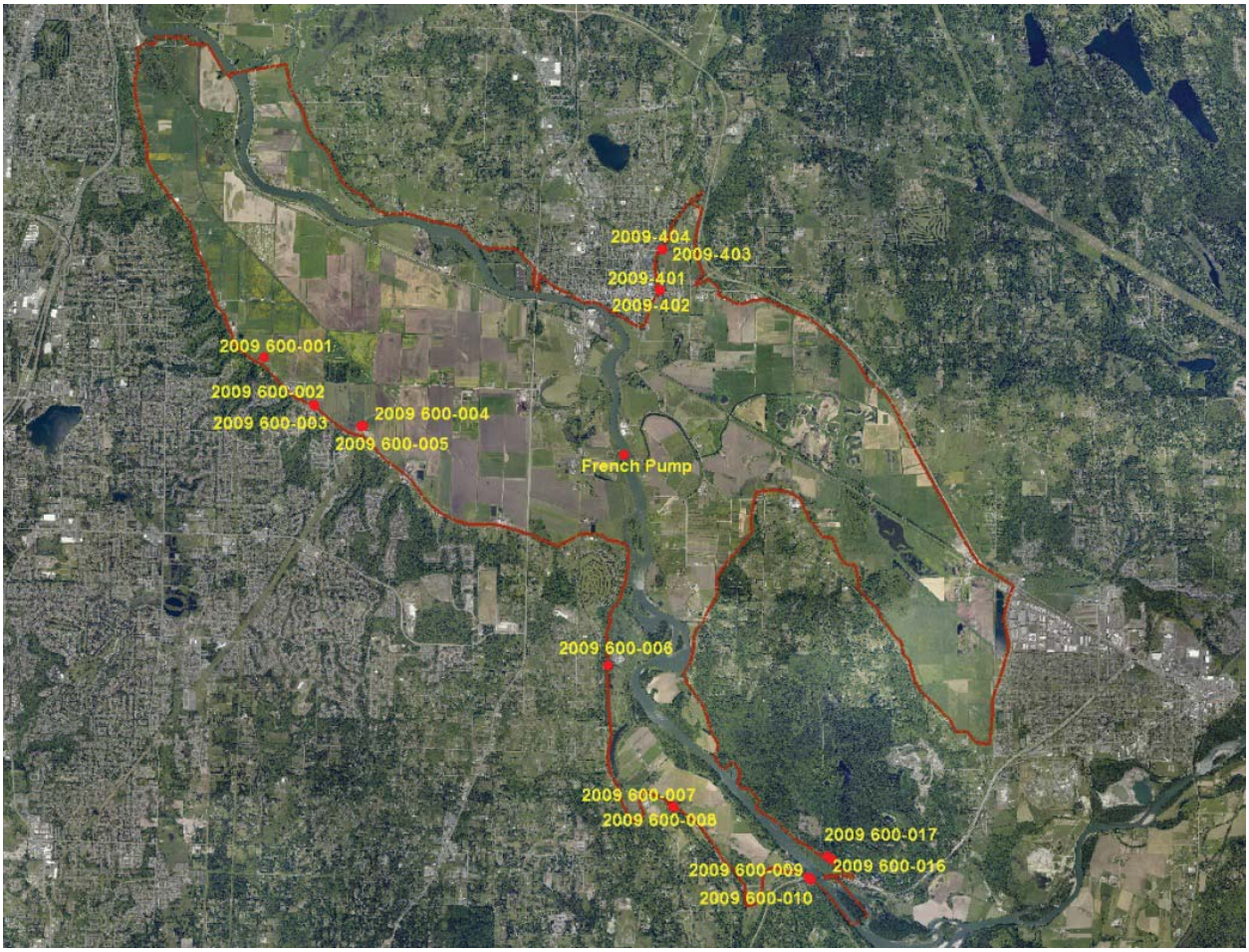

Figure 6. Locations of high water marks used as the basis for calibrating the 2D model.

Table 3 Coordinates and surveyed elevations at the HWM locations for the January 2009 flood event.

Point	Easting (ft)	Northing (ft)	HWM (ft, NAVD88)	Comment
2009-401	1333985	335555	36.41	u/s of 2nd St, left bank
2009-402	1333995	335529	36.44	d/s of 2nd St, left bank
2009-403	1334110	337603	38.57	d/s of 6th St, left bank
2009-404	1334106	337625	38.57	u/s of 6th St, left bank
2009 600-001	1313796	332122	16.64	Lowell-Larimer Rd near 44th Ave SE
2009 600-002	1316329	329703	15.39	Lowell-Larimer Rd near 56th Ave SE (A)
2009 600-003	1316380	329652	15.45	Lowell-Larimer Rd near 56th Ave SE (B)
2009 600-004	1318853	328637	15.99	near William Road (A)
2009 600-005	1318753	328604	15.54	near William Road (B)
2009-600-006	1331338	316415	35.29	Near Thomas Eddy
2009 600-007	1334647	309229	37.87	Elliott Road at 172nd St SE (A)
2009 600-008	1334692	309199	37.98	Elliott Road at 172nd St SE (B)
2009-600-009	1341703	305503	39.33	u/s of SR-522 Bridge, left bank
2009 600-010	1341574	305589	41	d/s of SR-522 Bridge, left bank
2009 600 016	1342780	306516	40.97	Tester Branch Road (A)
2009 600 017	1342539	306677	38.7	Tester Branch Road (B)

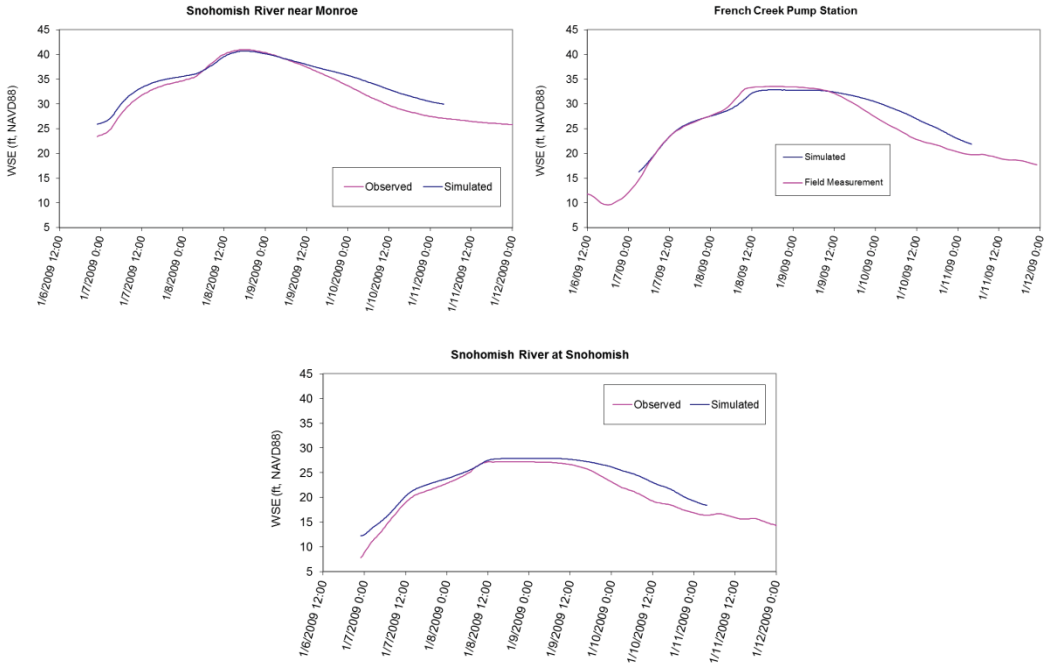

Figure 7. Comparison of predicted vs. observed WSEs at the three gage locations during the simulated January 2009 flood event.

Table 4 Measured and predicted HWMs for the January 2009 flood event. Adjacent HWMs are averaged, and the calibration errors are the differences between simulated WSEs and the average of proximal HWMs. A positive error means simulated WSE is higher, and vice versa.

Point	Easting (ft)	Northing (ft)	WSE (ft, NAVD88) HWM	WSE (ft, NAVD88) Calibrated	Calibration Error (ft)	Comment
2009 600-001	1313796	332122	16.64	15.60	-1.04	Lowell-Larimer Rd near 44th Ave SE
2009 600-002	1316329	329703	15.38	15.60	0.18	Lowell-Larimer Rd near 56th Ave SE (A)
2009 600-003	1316380	329652				Lowell-Larimer Rd near 56th Ave SE (B)
2009 600-004	1318853	328637	15.76	15.60	-0.16	near William Road (A)
2009 600-005	1318753	328604				near William Road (B)
2009-600-006	1331338	316415	35.29	35.41	0.12	Near Thomas Eddy
2009 600-007	1334647	309229	37.93	36.31	-1.62	Elliott Road at 172nd St SE (A)
2009 600-008	1334692	309199				Elliott Road at 172nd St SE (B)
2009-600-009	1341703	305503	40.17	40.31	0.14	u/s of SR-522 Bridge, left bank
2009 600-010	1341574	305589				d/s of SR-522 Bridge, left bank
2009 600 016	1342780	306516	39.83	39.32	-0.51	Tester Branch Road (A)
2009 600 017	1342539	306677				Tester Branch Road (B)

Validation

The calibrated model was validated against the November, 2008 flood event, which had a peak flow with approximately a 2-year return period. Although the 2008 event was smaller in terms of peak flow magnitude than the January 2009 event, the duration of high flow was longer. The inflow hydrographs of the Snohomish River and Pilchuck River used for model validation are shown in Figure 8 along with the WSE hydrograph for the downstream boundary. As for the January 2009 simulation, gaging station records were used to define the inflow time series, and the downstream boundary condition WSE hydrograph was provided by WEST Consultants (R. Walton, March, 10, 2014 email correspondence). To help the model obtain a suitable initial condition, the same spin-down procedure described in the calibration process was used where artificial hydrographs were specified for an 18 hour period preceding the start of the actual hydrographs (Figure 8).

The 2008 event simulation results indicated that only minor changes were required to Manning's n values established at selected locations during the calibration to the January 2009 event, to match peak water levels at the three gaging stations (i.e., SR-522 Bridge, French Pump Station, and City of Snohomish). For example, the channel Manning's n values below the City of Snohomish was changed from 0.03 (January 2009 flood) to 0.032 (November 2008 flood). There were no changes to roughness values between the City of Snohomish and the French Creek Pump Station. Upstream of the pump station, the range of Manning's n was changed from

0.032-0.038 (January 2009 flood) to 0.03-0.038 (November 2008 flood). In addition, only slight adjustments to marsh porosity properties were required for five element types located on banks or floodplains. In addition, only minor changes were required to element sink rates in the validation simulation. Since there were no HWMs available for comparison, the sink rates were designed to ensure the floodplain was nearly dry prior to the flood water overtopping the channel bank.

The fact that only minor changes were required overall gave us confidence that the January 2009 model predictions were reasonable. The resulting simulated hydrographs at the three gaging stations were reasonably close to the measured data (Figure 9), indicating the model was essentially validated and can be used in subsequent simulation of restoration or flood management scenarios.

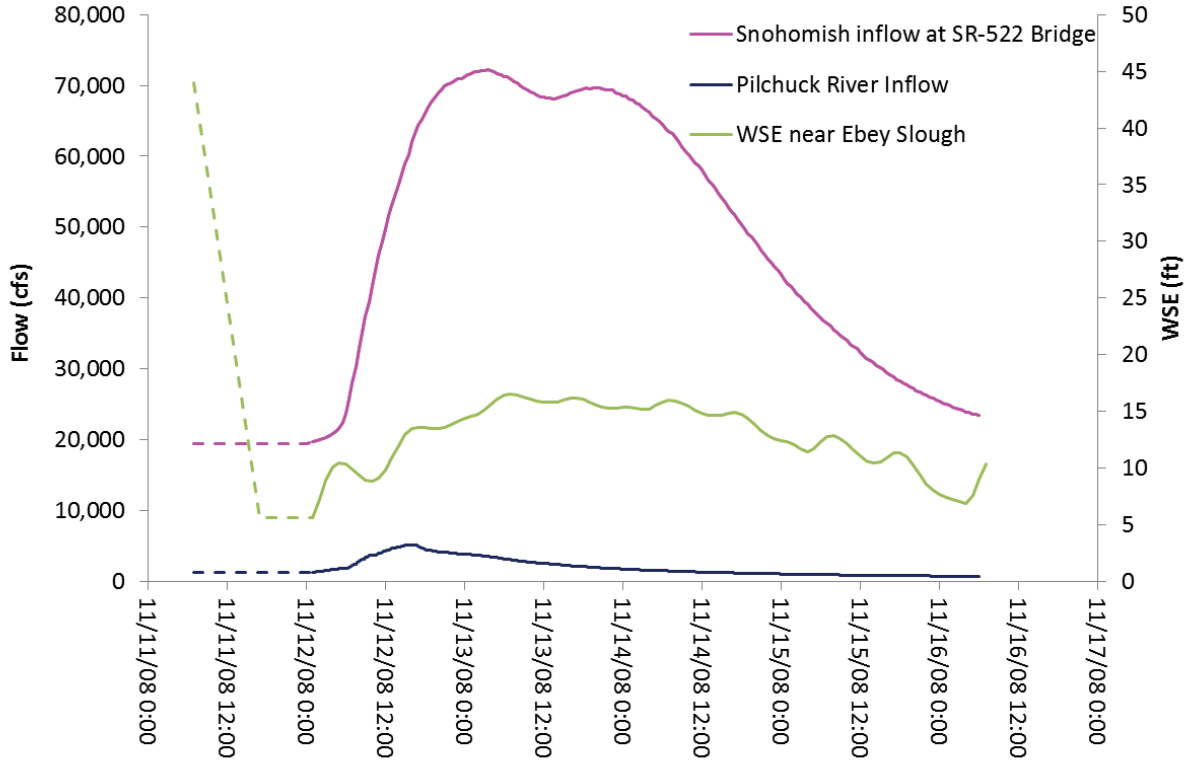

Figure 8. Hydrographs used in the simulation of November, 2008 flood.

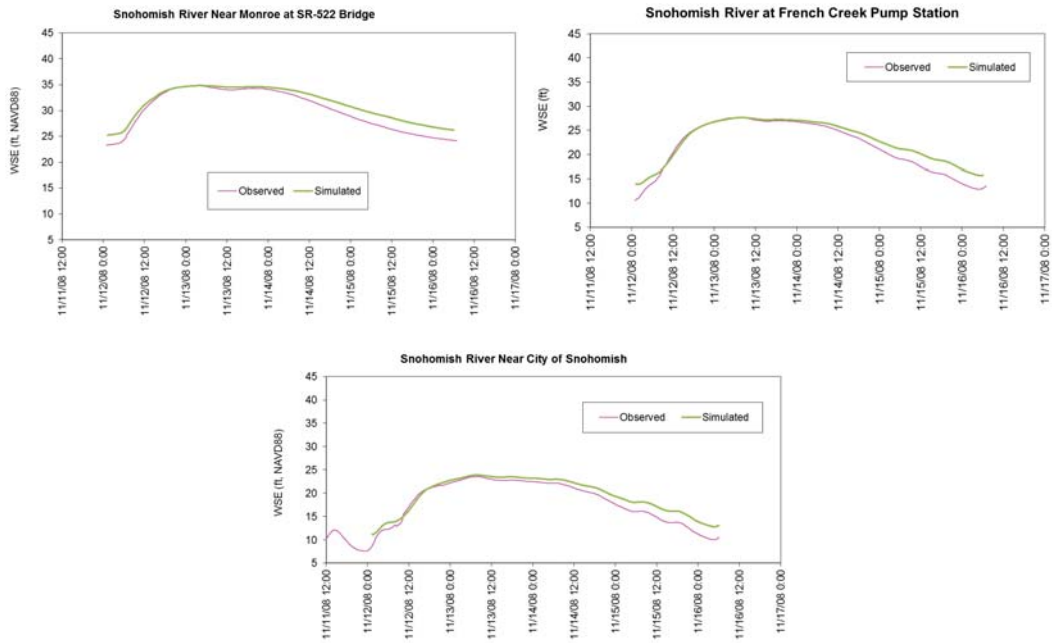

Figure 9. Comparison of predicted vs. observed WSEs at the three gages during the simulated November, 2008 flood event.

2.3 Sediment Transport Modeling

Sediment transport modeling involved using output from the calibrated 2D hydrodynamic model of the January 2009 flood event to predict sediment transport rates within the active channel, and develop a long term (i.e., over 50 years), within-reach sediment transport budget. The budget was represented by calculating a cumulative stream-wise variation in sediment trapping efficiency, which is the difference in net sediment transport volume coming into and out of a fixed segment of the river channel bounded by two cross-sections. Sediment transport rates accordingly were calculated at regularly spaced cross-section locations distributed along the length of the study reach, for a range of flow magnitudes and durations. The locations were defined every 1000 ft in GIS to define “analysis segments” (Plate 1; Table 5) for which sediment transport rates and other quantities such as bank migration rate could be calculated and compared spatially using a common framework irrespective of the extent to which channel planform changes might have occurred. This permitted a common framework for synthesizing the results from the various analyses.

In the sediment transport analysis, the length of analysis segments was increased to 2000 ft intervals in the reaches above and below the gravel-sand transition zone. Within the transition zone, where the riverbed grain size distribution fined rapidly in the downstream direction, the

analysis segment cross-section boundaries were maintained at the higher resolution 1000 ft intervals. This was done primarily for practical reasons, because the required hydraulic data for the analysis had to be extracted manually from the 2D model output. It was reasoned that a coarser resolution would suffice above and below the transition zone given that the grain size distributions were essentially constant and the channel was relatively prismatic within each sub-reach, such that upstream-downstream variation in bedload transport rates over consecutive cross-sections was likely to be more gradual than within the transition zone.

Table 5. River mile (RM) system used in the geomorphic analysis. Analysis segments were used to characterize spatial variation in sediment transport and deposition, and channel migration trends. RM convention follows current interpretation of Snohomish County's DFIRM database and is consistent with convention used by WEST Consultants' flood modeling work to date.

Analysis Segment	Analysis RM (Downstream Boundary)	Landmarks/Features
1	20.25	SR 522 Bridge
2	20.05	
3	19.85	
4	19.65	
5	19.45	
6	19.25	
7	19.05	
8	18.83	
9	18.62	
10	18.43	
11	18.25	
12	18.05	
13	17.86	
14	17.63	
15	17.35	
16	17.13	
17	16.92	Thomas' Eddy
18	16.68	
19	16.43	
20	16.17	Approximate Top of Gravel-Sand Transition Zone
21	15.96	
22	15.74	
23	15.52	
24	15.30	
25	15.10	
26	14.90	

Table 5. River mile (RM) system used in the geomorphic analysis. Analysis segments were used to characterize spatial variation in sediment transport and deposition, and channel migration trends. RM convention follows current interpretation of Snohomish County's DFIRM database and is consistent with convention used by WEST Consultants' flood modeling work to date.

Analysis Segment	Analysis RM (Downstream Boundary)	Landmarks/Features
27	14.70	
28	14.50	French Creek Pump Station
29	14.30	
30	14.12	
31	13.93	
32	13.74	
33	13.53	Pilchuck River Confluence
34	13.34	BNSF Bridge
35	13.15	
36	12.96	Old Rail Bridge
37	12.76	
38	12.57	99th Avenue Bridge
39	12.38	Approximate Bottom of Gravel-Sand Transition Zone
40	12.19	SR 9 Bridge
41	12.00	
42	11.82	
43	11.64	
44	11.45	
45	11.25	
46	11.06	Fields Riffle (Mud Bay)
47	10.87	Fields Riffle (Mud Bay)
48	10.68	
49	10.48	
50	10.30	
51	10.11	
52	9.93	
53	9.74	
54	9.54	
55	9.36	
56	9.17	
57	9.00	
58	8.82	
59	8.64	Norwegian Bay
60	8.44	Norwegian Bay
61	8.25	
62	8.06	Head of Ebey Slough

2.3.1 Sediment Transport Simulation Flows

The 2D model was calibrated for an unsteady flow event, and the reach experiences numerous sources of variability influencing hydraulic simulations including tidal cycling and stage-flow hysteresis effects associated with large low gradient rivers. It was accordingly not feasible to simulate all flood hydrographs over a 50 year period, thus a simplified approach was followed where a range of flows was selected from the calibrated January 2009 event simulation, and the hydraulic properties associated with those flows were taken as representative of general conditions influencing sediment transport rates in the river. The simulation flows were selected to cover the range of discharges associated with significant bedload transport in the gravel and gravel-sand transition zones that occurred during the January 2009 event, from the 5 percent exceedance flow to the peak flood which corresponded approximately to the 20 year flood event (Table 6). The 5 percent exceedance flow was selected as the lower bound to the analysis flows because relatively little bedload transport occurs in general in alluvial rivers when discharge is below that level (Schmidt and Potyondy 2004). The upper limit reflected the peak flow magnitude in the calibrated 2D model, and the results for the 20 year flood were taken in the trapping efficiency calculations to also approximate the transport rate at higher flood levels up to the 50 year event level given that flood flows are fully overbank at the 20 year level (the dikes are generally estimated to contain flood flows between the 5- and 10-year event levels).

Each flow in Table 6 was assigned a duration over the 50 year period such that the number of days added up to 913 (equivalent to ~5% of a 50 year period). The number of days for each level was determined iteratively while attempting to match the shape of the duration curve and the cumulative flow volume underneath the curve (Figure 10). The selected number of flows in Table 6 reflected a pragmatic, subjective balance between time to extract the requisite hydraulic data from the 2D model output (fewer steps desired) and analysis resolution and accuracy (more steps desired, where a closer match could have been achieved in Figure 10 by adding more steps in the discretized curve).

Table 6. Simulation flows for which shear stresses were computed in the sediment transport analysis using hydraulic data extracted from the 2D hydrodynamic model. The resulting predicted total transport rate over the active channel bottom was multiplied by the duration and summed across flows

Flow ID	Percent Exceedance	Duration (days)	Flow (cfs)
PF1	5	490	23890
PF2	1	264	43200
PF3	0.5	66	52907
PF4	0.4	25	56195
PF5	0.3	24	60543
PF6	0.2	23	65228
PF7	0.1	14	72400
PF8	0.03 (~10-yr flood)	4	114000
PF9	0.014 (~20 yr flood and higher)	3 (including larger floods)	132000

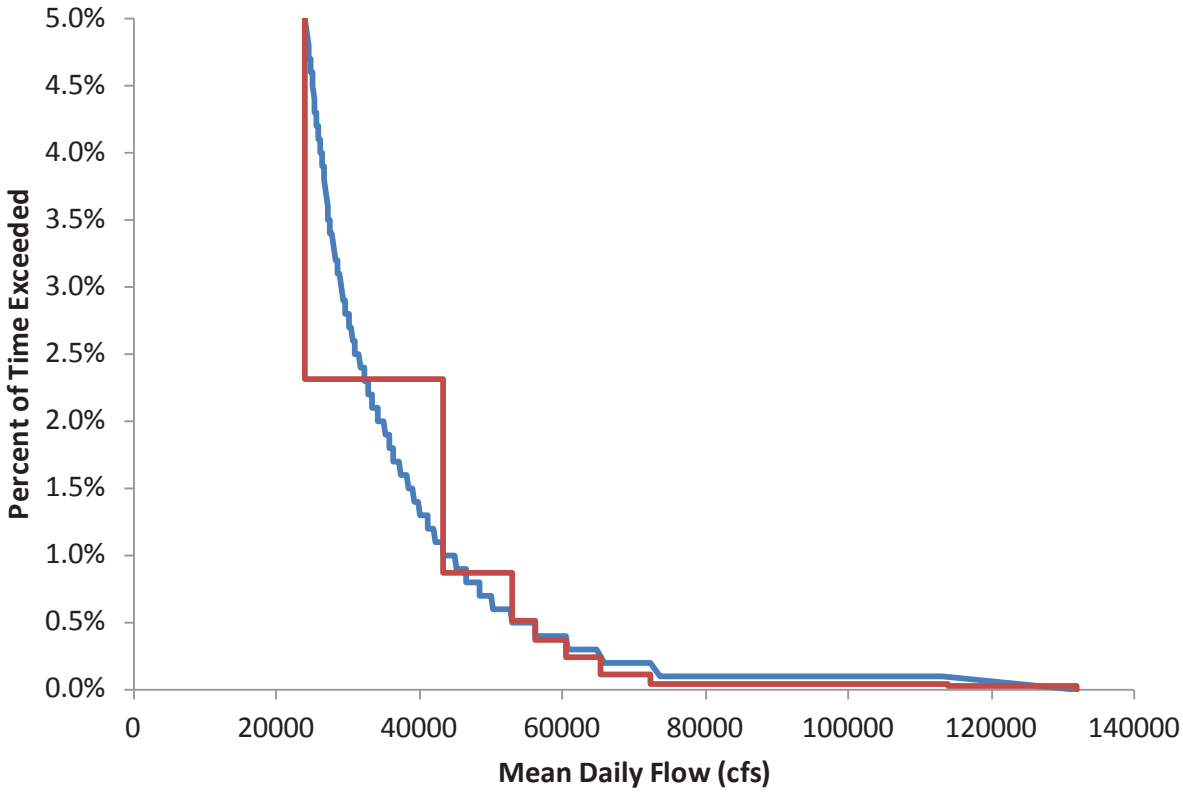

Figure 10. Flow duration curve developed for the analysis reach using the mean daily flow record at USGS Station # 12150800, and corresponding discretization employed to approximate flow duration for the 50-year bedload transport sediment trapping efficiency calculations.

2.3.2 Long Term Sediment Trapping Efficiency Analysis

The long term tendency for vertical stability of the riverbed was evaluated by computing cumulative bedload transport volumes over a 50 year period at the cross-sections defining analysis segments. A 50-year period was simulated to correspond to a representative project design life. Transport volumes were calculated for every cross-section in Table 5 falling within the gravel-sand transition zone, and for every other cross-section above and below the transition zone. A variety of sediment transport equations were applied and the results compared to see if spatially consistent patterns of predicted aggradation, degradation, or an approximately neutral tendency were predicted over the long term.

The RMA2 model has a sediment transport add-on module (SED2D) available, but it is only capable of simulating transport of a single grain size (i.e., effectively sand bed). The sediment transport calculations occur essentially 'within the box' and are thus difficult to evaluate. Greater flexibility and control was obtained in this analysis by post-processing hydraulic output outside of RMA2, and applying four different sediment transport equations to provide independent estimates of transport rate:

1. Engelund and Hansen (1967) total load equation;
2. Ackers and White (1973) total load equation;
3. Yang (1973) total load equation; and
4. Wilcock and Crowe (2003) equation for gravel and sand bedload.

All four equations were selected because they relied on hydraulic parameters that could be derived relatively easily from the 2D model output. The three total load equations were used because of their relative simplicity and capacity to model gravel and sand sized particles. The Wilcock and Crowe (2003) equation was applied to the gravel-sand transition zone and upstream only because it was developed for gravel-sand mixtures; the application of this equation ignored suspended sediment transport by inherently assuming that the gravel river bed elevation was most substantially influenced by gravel transport and deposition.

Predicted hydraulic parameters were accordingly extracted from the 2D model output to calculate shear stresses in the main channel at each flood level listed in Table 6. Two alternative estimators of shear stress (τ) were computed and input to the sediment transport analysis:

1. Uniform depth approximation: $\tau = \rho g R S$

where ρ = density of water, g = acceleration due to gravity, R = hydraulic radius (approximated by predicted depth), and S = energy slope (approximated by predicted local water surface slope); and

2. Roughness-based relation of shear velocity to mean column velocity (cf. Richards 1982):

$$\frac{V}{u^*} = 5.75\, log\left(\frac{H}{D_{65}}\right) + 6.00$$

where $u^* = \sqrt{\tau/\rho}$ = shear velocity, V = mean column velocity, H = flow depth, and D_{65} = the particle size on the riverbed for which 65% of the surrounding material is smaller than.

For the uniform depth approximation, values of R were derived by calculating the approximate conveyance area divided by the wetted perimeter within the portion of the channel bed considered mobile, and values of S were approximated using the longitudinal water surface elevation slopes. For the roughness-based estimator, values of V and H for a given flow level were extracted from the model output at nodes across the active river bottom at each cross-section location and averaged over the active/mobile portion of cross-section.

The shear stress estimators yield different magnitude results for shear stress, where the roughness based relation yields a considerably smaller estimate than the uniform depth based relation, to the point that the former tended to underestimate gravel transport rates in the upper portions of the assessment reach. Sediment transport rates calculated for any given transport equation therefore could not be compared directly across shear stress estimators. However, by calculating sediment transport rates consistently and independently using the same shear stress estimator, it is possible to compare relative changes in long term sediment trapping efficiencies where only the cumulative tendency (for aggradation, degradation, or equilibrium) is the metric. Therefore, there were two independent sets of trapping efficiency results generated for each sediment transport equation, and greatest confidence in interpreting the results occurred where the two sets of results indicated similar vertical stability tendencies.

The results were used to characterize analysis segments within the reach regarding their deposition or erosion tendencies, which in turn served as a guide to the type of project that may or may not succeed in the segment. For example, fish habitat structures constructed using large wood would not be expected to succeed in an analysis segment that was predicted to strongly

experience a net gain in sediment over time, because the structures would have a higher risk of burial or abandonment by the river.

The roughness-based relation shear stress estimator and all bedload transport equations required input data describing riverbed grain size. Inspection of the longitudinal scatter in D_{50} and D_{90} values (see Results, Section 3.1) indicated that there were three sub-reaches in the plot corresponding to large scale breaks in grain size, reflecting an upstream gravel bed, a downstream sand bed, and a gravel-sand transition zone between. The resulting three grain size distributions were applied to subsections of the reach modeled in the sediment transport analyses.

Sediment trapping efficiency was computed for each flow in Table 6 and analysis segment by estimating sediment transport rates at the bounding upstream and downstream cross-sections, and applying a mass balance equation for bed elevation change between cross-sections as a function of estimated input and output bedload mass transport rates per unit width (q_B), active width (W), distance between cross-sections (L), sediment density (ρ_s), and porosity (P) (DeVries 2000):

$$Y_T = \int_{t1}^{t2} \frac{\partial Y}{\partial t} dt \cong -\sum_{t1}^{t2} \left[\frac{(q_B W)_{out} - (q_B W)_{in}}{0.5L(W_{in} + W_{out})\rho_s(1-P)} \right] \Delta t$$

where the incremental change in bed elevation ($\partial Y/\partial t$) was evaluated for each simulation flow and then multiplied by the histogram time increment (Δt) over which the modeled flow occurred during the 50-year period (cf. Figure 10). This was repeated for other flows, and the results summed to estimate a net mean change in bed elevation Y_T between successive cross-sections. The active width was derived from the bathymetry data in confined sections (= most of the assessment reach) and from scaled aerial photographs in wider sections located upstream. A strongly positive value of the $\partial Y/\partial t$ sum was inferred as an indication of a strong tendency towards aggradation, and a strongly negative value as an indication of a stronger tendency towards degradation.

Seven aggradation/degradation potential classes were developed subsequently and used to characterize deposition trends based on the sign and magnitude of the predicted bed elevation change, with magnitudes varying depending on transport equation (Table 7). Each set of classes was developed using professional judgment based on the range of plots of predicted changes for an analysis segment against its downstream boundary river mile. Each analysis segment was classified accordingly and the results depicted graphically in ARC-GIS.

Table 7. Predicted bed elevation change rate and sign used to classify analysis segments according to sediment transport and deposition characteristics in the Snohomish River.

Vertical Stability Tendency		Bed Elevation Change Rate (ft/yr) by Transport Equation			
Class	Potential	Engelund-Hansen	Ackers-White	Wilcock-Crowe	Yang
1	High Degradation	< -3.5	< -1.0	< -1.0	<-5
2	Moderate Degradation	-3.5 to -2.0	-1.0 to -0.2	-1.0 to -0.2	-5 to -3
3	Mild Degradation	> -2.0 to < -0.5	> -0.2 to < -0.05	> -0.2 to < -0.05	>-3 to <-1
4	Neutral/Equilibrium	-0.5 to 0.5	-0.05 to 0.05	-0.05 to 0.05	-1 to 1
5	Mild Aggradation	> 0.5 to 2.0	> 0.05 to 0.2	> 0.05 to 0.2	>1 to 3
6	Moderate Aggradation	> 2.0 to 3.5	> 0.2 to 1.0	> 0.2 to 1.0	>3 to 5
7	High Aggradation	> 3.5	> 1.0	> 1.0	>5

2.4 Aerial Photograph Interpretation

Channel features were digitized from mosaicked and georeferenced aerial photographs, spanning from 1933, 1947, 1955, 1965, 1974, 1984, 1991, 1998, 2001 and 2011. Results from 1998 were not used in the final analysis as there were negligible changes evident between 1991 and 2001; this kept comparisons between successive years over approximately similar intervals. The analysis segments listed in Table 5 and depicted in Plate 1 were defined in GIS, and spatial and temporal patterns in channel migration rate and gravel bar area were derived from the aerial photographs to infer relative lateral stability of each analysis segment.

2.4.1 Historic Channel Planform Mapping

Right and left river bank locations were digitized by the SWM GIS staff for each year of photographs. The left and right banks of the river channel and visible side channels were mapped. The resulting digitized poly lines were overlaid chronologically and locations compared between consecutive sets of photographs. Migration rates were estimated as the local average offset distance within an analysis segment between successive main channel river bank traces, divided by the number of years between the two sets of photographs. The calculated migration rates were used as the basis for classifying an analysis segment according to planform changes, using rates established in previous analyses for the Skykomish, Sauk, and Stillaguamish rivers (Table 8). The riverbank with the greater average annual migration rate was used to classify a segment.

Table 8. River channel migration rate classification for assessing channel planform changes. Migration may be to either left or right bank directions.

Planform Change Index	Average Migration Rate (ft/yr, one or both banks)
1	< 15 (minor change/measurement error)
2	15-30 (small change)
3	30-80 (moderate change, wandering tendency)
4	>80 (severe change, braiding tendency)

2.4.2 Gravel/Sand Bar Area Mapping

Exposed, unvegetated (i.e., active) main channel gravel/sand bar areas were digitized from the aerial photographs as discrete polygons when visible. The area of gravel bar mapped in each segment was then computed and summed cumulatively from upstream to downstream to reflect the direction of sediment transport and deposition. The results were also referred to in some cases for verification of the location of the right or left riverbank during calculation of migration rates.

2.5 Avulsion Potential Assessment

Avulsion potential was assessed using LiDAR topographic data collected in Spring 2006, 2D flood modeling results, and various GIS data. Factors evaluated as contributing to the potential for avulsion included the presence of concentrated flow pathways evident on the topographic surface, the average slope of pathway segments, the general flow level at which the upstream inlet would be inundated, and the inherent erosivity of soils associated with the pathway. Potential factors that could reduce the potential for avulsion were also identified, including vegetation and the presence of infrastructure. The methods used to characterize and identify these various factors are described below.

2.5.1 Individual Avulsion Potential Factors

Flow Paths: Potential avulsion pathway segments were traced on 2 ft contour maps generated from the County's LiDAR data as linear features following topographic routes of low points on the floodplain. Segments began and ended at the main river channel or junctions with other segments. A GIS layer was then constructed by Sheila Hagen (SWM GIS staff) that depicted each potential pathway segment as a linear feature.

Inundation Flow Level: The inlet control elevation of pathway segments branching from the river was used to estimate the return interval event at which each segment and connected

segments downstream and upstream would become wetted, using water surface elevations estimated for the 2-year, 10-year, and 20-year event based on the 2D hydrodynamic modeling of the January 2009 event. Where the inlet crossed an existing dike, the crest elevation of the dike was identified from survey data for evaluating overflow level under current conditions, and the adjacent ground elevation was extracted from the LiDAR data for evaluating engagement flow level if the dike were ever to be set back in the future. Segments below junctions with upstream segments were assumed to be connected at the same level as upstream segments as long as there was no significant break in slope evident on the map downstream. For example, if a downstream segment was connected to two upstream segments with one flowing at the 2 year flood level and the other at the 10 year flood level, the downstream segment was assigned a 2-year flood level engagement.

Slope: A longitudinal profile for each pathway was developed by extracting elevations from the LiDAR data for selected points spaced 100 ft apart along each segment. Average slope was calculated as the average of slopes calculated between points, for each segment. Slope between points was calculated as the difference in elevation between points divided by the length between points (100 ft or shorter, depending on the total length of the segment).

Soil Erodibility: The avulsion pathway layer was overlaid in GIS on a soils map produced by the Natural Resources Conservation Service (NRCS). Each soil type is assigned a K_w-factor which represents both susceptibility to erosion and the infiltration rate. Soils with lower K_w-factors are more resistant to erosion due either to high clay content or high infiltration. Soils with higher K_w-factors are more erodible. Soils within the study area were classified as follows based on the NRCS K_w-factor, with greater emphasis placed on the uppermost soil horizon:

1 = K_w-factor > 0.3 (higher erodibility)
2 = K_w-factor 0.2-0.3 (moderate erodibility)
3 = K_w-factor <0.2 (lower erodibility)

Where potential avulsion pathways crossed soils with different K_w-factors, a weighted average class was calculated based on the relative length of channel crossing each soil type.

Vegetation Cover: In general, the presence of forest vegetation is anticipated to reduce the potential for avulsion, as trees provide deep, dense root masses that are more resistant to erosion and may inhibit braiding (Miall 1977). In addition, if channels do avulse through forested areas, trees that fall into the new channel provide roughness elements that reduce erosive energy and

may temporarily block flow. However, given that most of the floodplain is used for agriculture and not forested, this factor was not considered further in this assessment.

Road Grade Controls: The presence of roads can act as both a mitigating factor or exacerbate the potential for avulsion. Paved roads, and to a lesser extent gravel roads represent a "hard point" that is more resistant to erosion over the short-term. However, roads that cross avulsion pathways may also exacerbate the potential if they contain undersized drainage structures or temporarily hold back water then fail catastrophically. This analysis assumes that roads are monitored and/or protected during floods and thus moderate the potential for avulsion where they are present. Road crossings were identified from the 2011 aerial imagery. Paved roads were considered to be more resistant and more likely to be protected during floods, and thus were assigned a greater mitigative factor.

Bank Hardening: The presence of bank hardening can retard avulsion if the river does not erode around the structure and it is designed and built to counter the potential for undermining at the bank toe. A majority of the reach banks have been hardened in one form or another. Avulsion potential therefore needs to be evaluated on a case-by-case basis, where type of structure (i.e., rip rap or LWD), condition of the structure, distance from the upstream and downstream ends of the structure to a floodplain swale, and respective structure end point and swale elevation differences can either be a mitigating factor or not substantially affect avulsion potential depending on the particulars of the site. For that reason bank hardening was not explicitly included as a factor in this reach-scale avulsion potential analysis.

2.5.2 Joint Avulsion Vulnerability Factors

The factors above were considered for ways to combine them into a joint avulsion vulnerability rating system. Weighting factors were conceived and assigned to ranges of each factor. It was decided to combine the flow level, slope, and soil erodibility factors into a weighted joint vulnerability rating system, and apply vegetation and road characteristics as mitigating factors. Each pathway segment identified on the LiDAR topographic surface was rated accordingly, following the gradations and weightings proposed in Table 9. The joint avulsion vulnerability was calculated for each segment as the sum of the weights assigned in Table 9 for return interval event at which the pathway may flow, pathway slope, and soil erodibility. The following joint classes were then defined based on professional judgment:

- Joint Vulnerability Weight Sum >14 = Class 1 (highest risk)
- Joint Vulnerability Weight Sum = 10-14 = Class 2

- Joint Vulnerability Weight Sum = 6-10 = Class 3
- Joint Vulnerability Weight Sum <6 = Class 4 (lowest risk)

Mitigating factor ratings can be used on a case-by-case basis in consideration of greater site specific knowledge as to the relative importance each factor could play in mitigating joint avulsion vulnerability.

Table 9. Summary of parameters used to assess relative avulsion potential, and the weights assigned to each parameter.

Risk Factors	Criterion (weight)			
Flood Return Interval Causing Inundation	>100 yr (1)	100 yr (3)	10 yr (6)	2 yr (9)
Slope	≤0% (1)	0-1% (3)	1-3% (6)	>3% (9)
Soil Erodibility Class	3 (1)	2 (2)	1 (3)	

3. RESULTS

3.1 Longitudinal Profiles

The grain size data from the Snohomish River channel indicate the presence of three distinct large scale morphologic reaches: an upstream section composed of gravel with relatively little cobble present, a gravel-sand transition zone, and a sand bed section downstream (Figure 11). The data upstream of RM 15 were based on bar surface pebble counts performed in 2000, whereas the data downstream are from the 2013 Ponar samples. Despite differences in methodology, the results are generally consistent spatially, with the possible exception of the most upstream Ponar sample where a greater amount of gravel on the riverbed surface was apparent to the touch during Ponar deployment and retrieval. The gravel interfered with proper operation of the sampler, requiring many attempts before settling on a reduced sample weight compared with downstream samples.

The longitudinal elevation profile of the Snohomish River thalweg is approximately linear above and below the gravel-sand transition zone in the steeper (S=0.0008) and less steep (S=0.00023) gravel and sand bed reaches, respectively (Figure 11). The slope of the gravel-sand transition zone (S=0.0010) is most similar to the slope of the gravel bed reach upstream. Regression lines of thalweg elevation in the gravel and sand bed reaches cross in the middle of the gravel-sand transition zone, between the French Creek Pump Station and the mouth of the Pilchuck River, when extended downstream and upstream, respectively. The grain size distributions are accordingly relatively similar within the respective reaches, reflecting the approximately linear bed slopes. The generally linear profiles and consistent grain size distributions suggest that the gravel-bed and sand bed reaches are in approximate equilibrium overall with respect to bedload transport capacity.

The approximate upstream extent of tidal influence during low flow is evident in Figure 11, with mean tide level (MTL) and mean higher high water (MHHW) approaching riverbed elevation at around Thomas' Eddy (~RM17). However, this tidal effect becomes less influential on water levels as the river flow increases, and thus has little apparent effect on sediment transport and deposition patterns. Review of flow records for the USGS' Snohomish River at Snohomish gage (Station #12155500) indicates that tidal cycling in the hydrograph disappears when flows exceed around 35,000 cfs at the Monroe gage (Station #12150800), which is around the 2% exceedance level (cf. Figure 10).

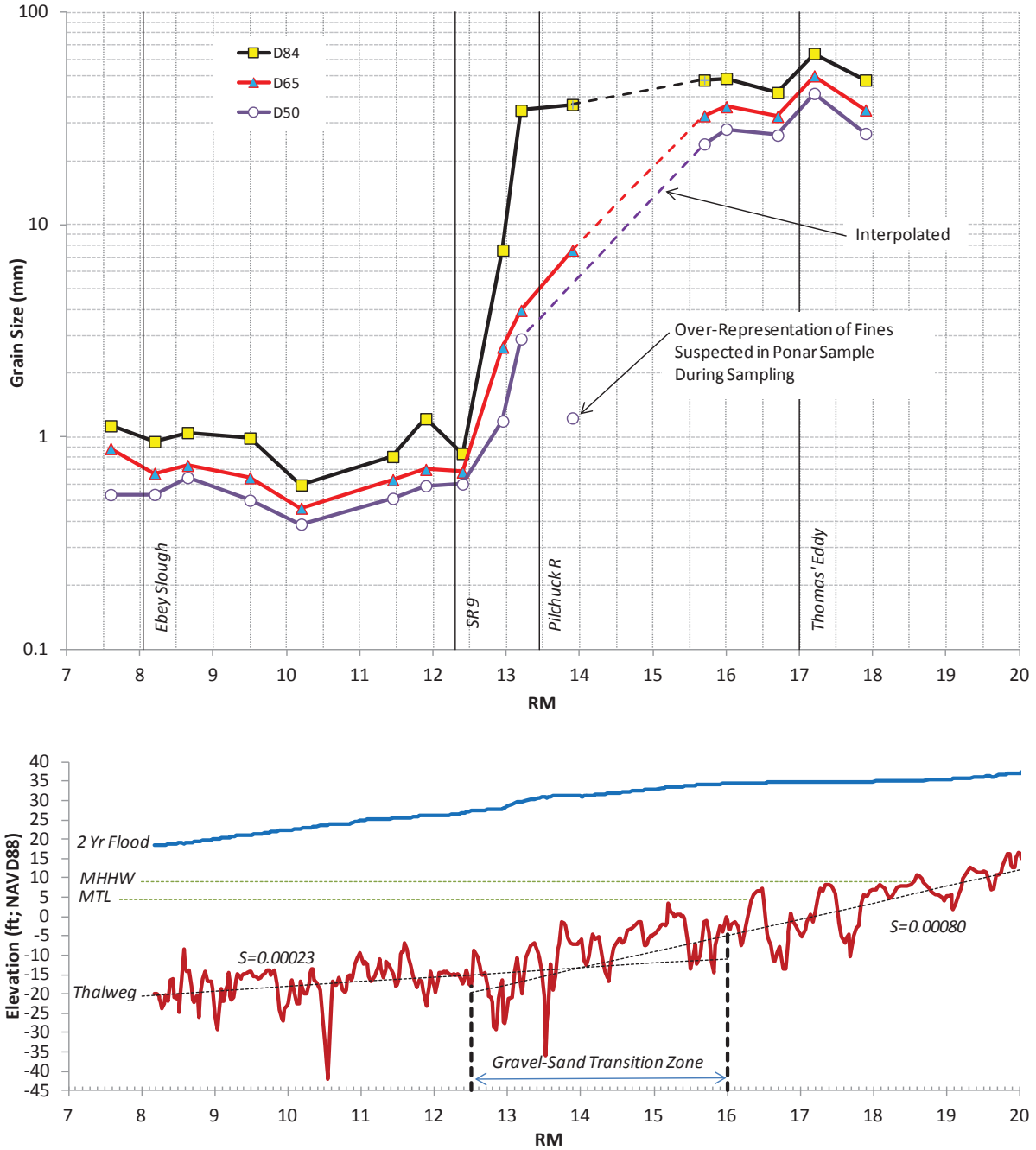

Figure 11. Longitudinal thalweg elevation, peak WSE profile during the January 2009 event, and variation in selected grain size distribution (GSD) percentiles measured in the Snohomish River. Typical tidal range is also depicted. Bed and 2-year flood elevations were extracted from the 2D model. Interpolation was relied on for describing missing grain size data in the sediment transport modeling.

The grain size distributions in Figure 11 are from the surface of the riverbed at low flow. It is unknown whether gravel extends farther downstream of RM ~12.5 at lower elevations in the bed, but it is possible because gravel from upstream has to settle somewhere in the reach. Comparison of long profiles from circa 1988 and the bathymetry data collected for this assessment indicate that the bed appears to have risen most consistently in the central portion of the gravel-sand transition zone above the Pilchuck River (Figure 12). This general location is where the thalweg regression slopes in Figure 11 cross, and future aggradation in this subreach is expected based on the longitudinal profile characteristics.

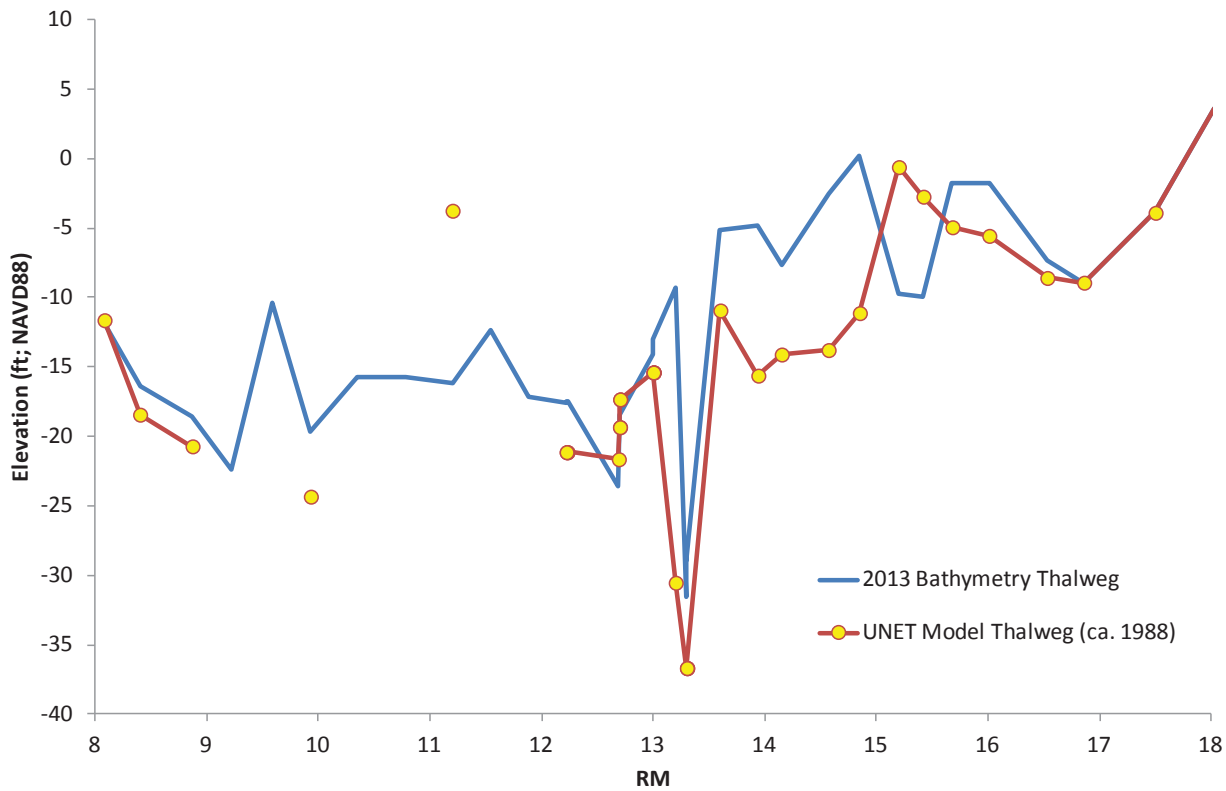

Figure 12. Comparison of longitudinal thalweg elevation profiles measured in the Snohomish River in 2013 and ca. 1988 (data in plot provided by Ray Walton, WEST Consultants).

3.2 Calibrated Hydrodynamic Model Output

The 2-dimensional hydrodynamic model covers a large area of approximately 22 square miles, and this posed limitations on the resolution of the model mesh because of computing time constraints associated with numerical modeling. Accordingly, the resolution of the model was

set up to represent large scale flow patterns over the model domain, with coarsest resolution over the floodplain and finest resolution within the channel and in the vicinity of significant topographic features. The model was not set up to simulate flow patterns accurately at small, hydraulic structure length scales (e.g., at small openings under the BNSF railway track). Nonetheless, the spatial and time step resolutions of the model were sufficient to provide results that could be used to infer hydraulic properties influencing geomorphic processes acting at the channel-width length scale. Examples of model output for around the time that peak stage occurred at the mouth of the Pilchuck River in the January 2009 event simulation are provided in Figures 13-15 for velocity contours, velocity directions, and water depth contours, respectively.

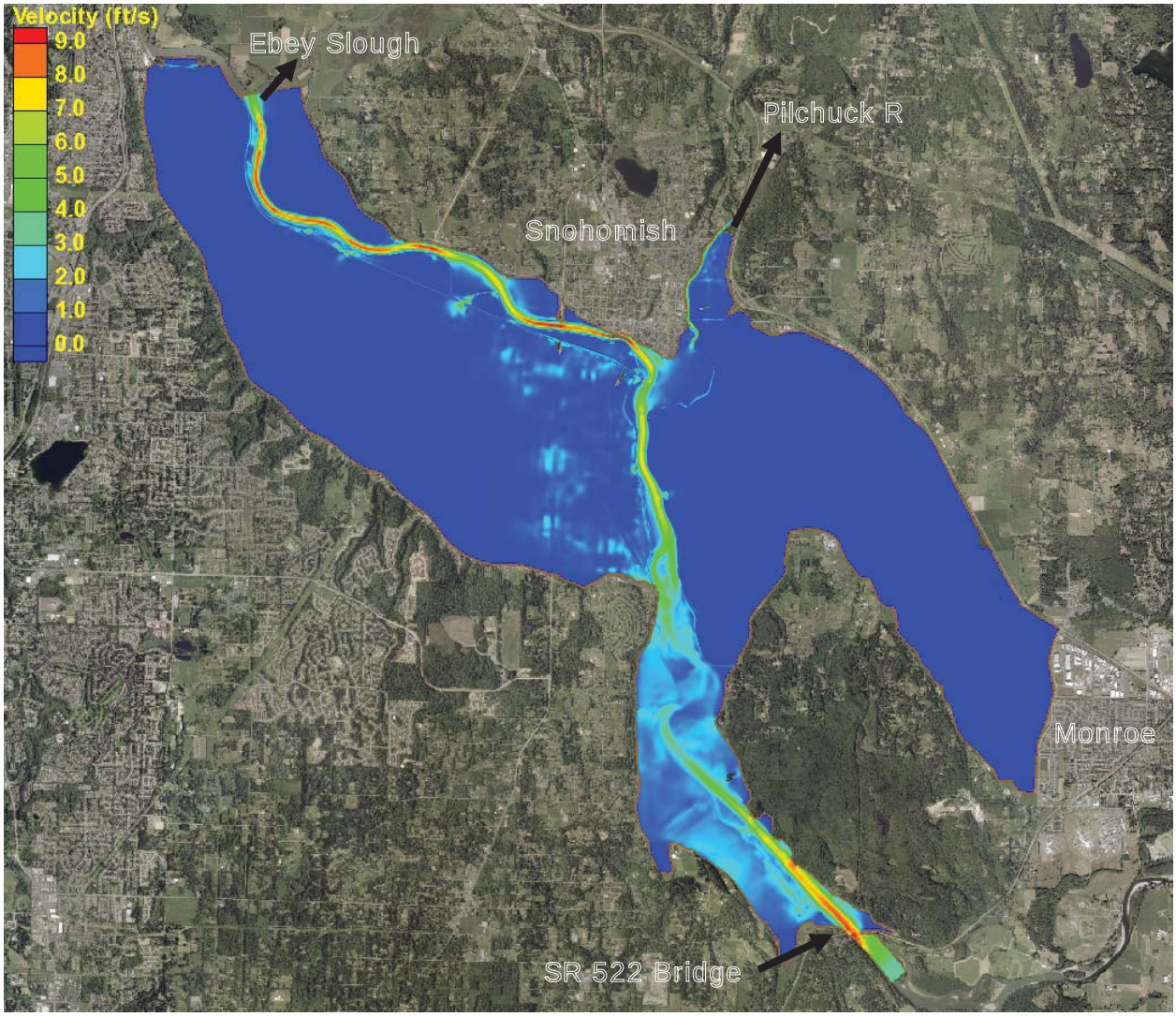

Figure 13. Predicted velocity distribution around the time of peak WSE (T=73.4 hours) near the mouth of the Pilchuck River during the January 2009 event.

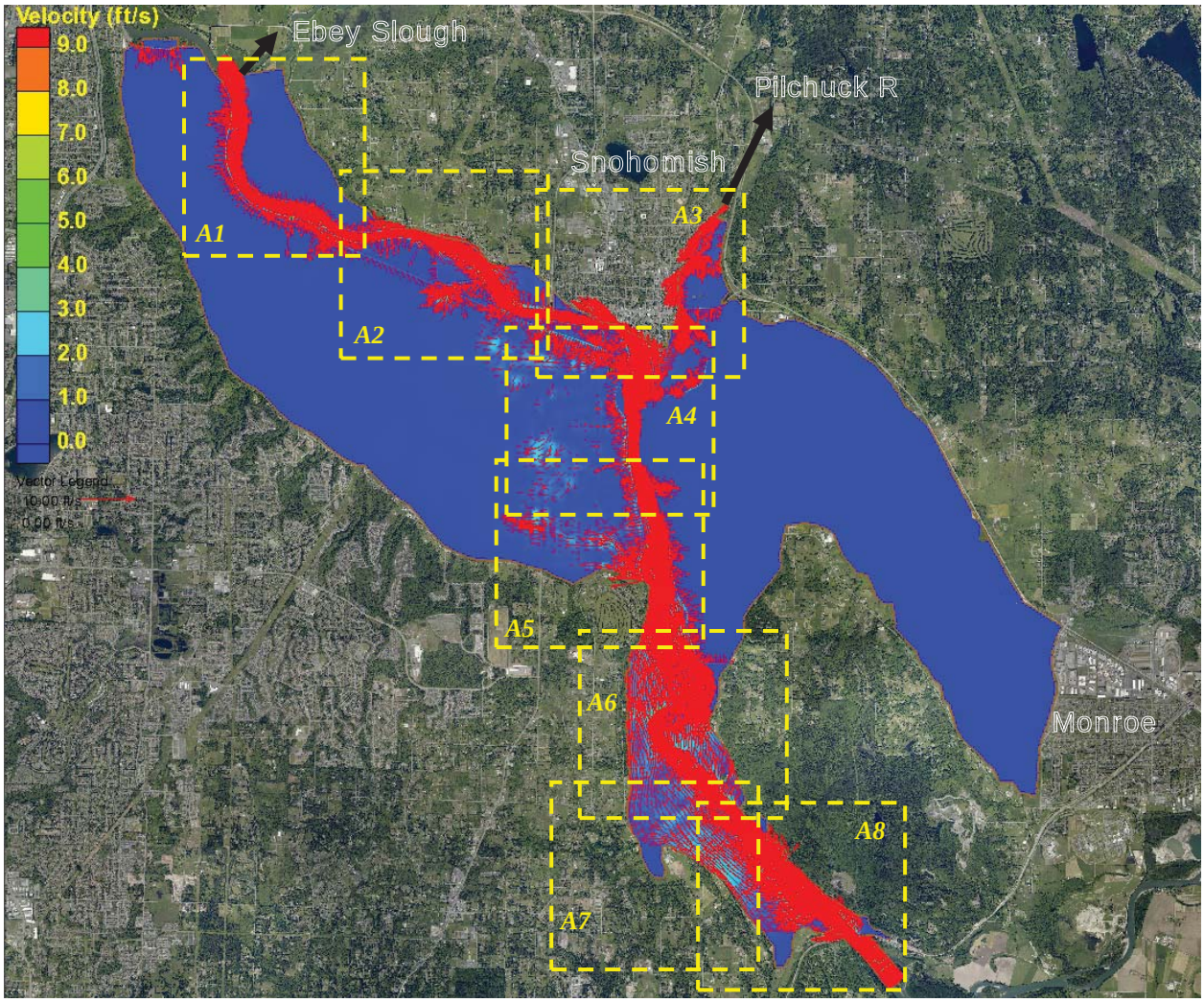

Figure 14. Predicted velocity magnitudes and directions at selected locations around the time of peak WSE (T=73.4 hours) near the mouth of the Pilchuck River during the January 2009 event. The boxed areas A1-A8 are presented in greater detail in Appendix A.

3.3 Sediment Transport Modeling

Predicted magnitudes of long term bed elevation changes varied considerably for the same location depending on which equations were used to estimate (i) shear stress and (ii) bedload transport rate. The shear stress estimates resulting from the uniform depth approximation were nearly an order of magnitude greater than the estimates from the roughness relation, and accordingly, the predicted sediment transport rates and corresponding absolute levels of bed change were greater for the former. And, in the cases of both the uniform depth approximation (Figure 16) and roughness-based relations (Figure 17) for shear stress, the magnitude of the

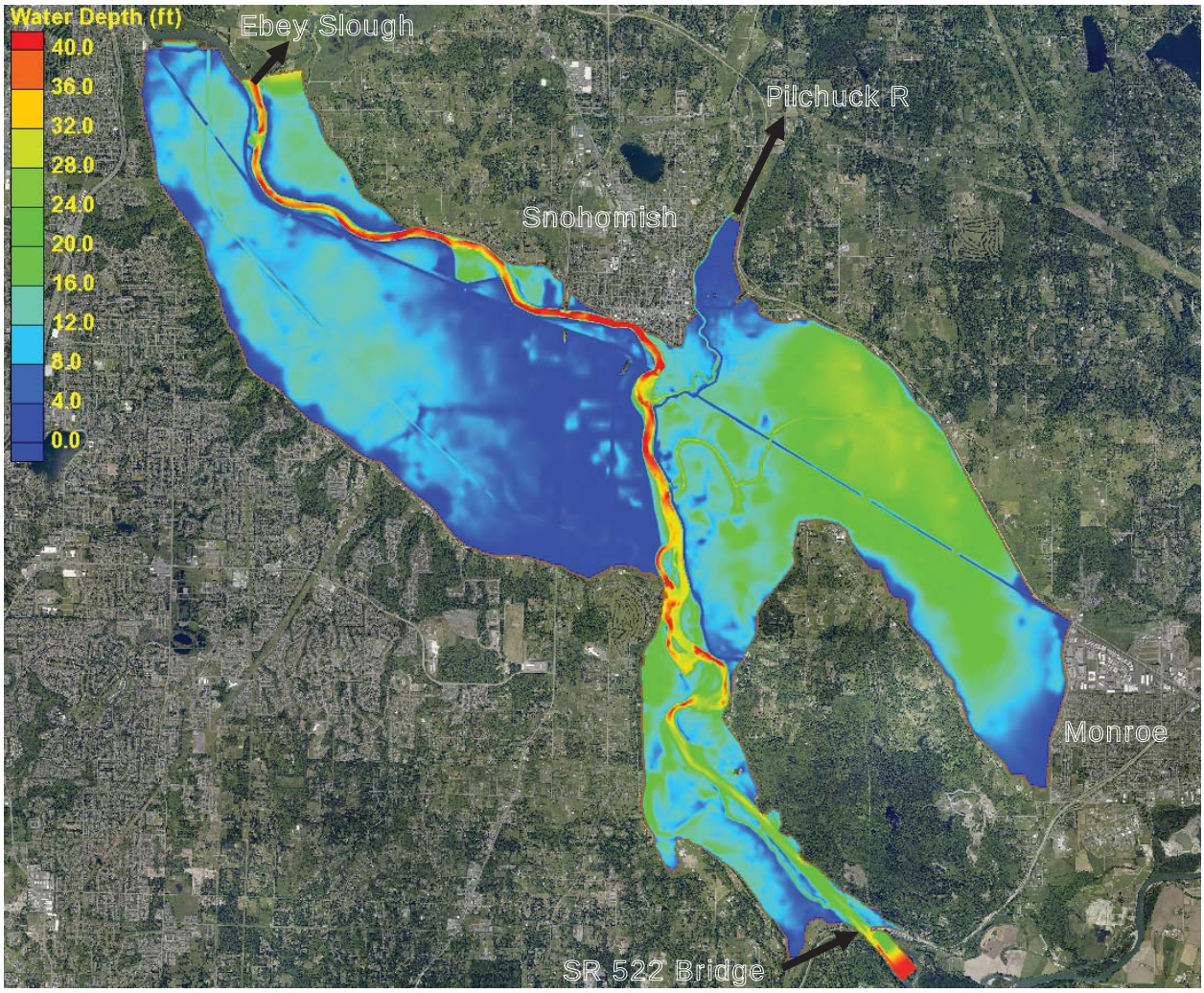

Figure 15. Predicted depth distribution around the time of peak WSE (T=73.4 hours) near the mouth of the Pilchuck River during the January 2009 event.

predicted bed elevation change at a location varied considerably depending on the sediment transport equation used and whether the location was upstream, within, or downstream, of the gravel-sand transition zone. The Wilcock-Crowe (2003) equation was most applicable of the four equations to gravel bed channels, whereas the Engelund and Hansen (1967) and Ackers and White (1973) equations were more applicable to sand bed channels; indeed, the latter predicted no transport in the gravel bed reach, which is not reasonable. The Yang (1973) equation appeared to yield more reasonable results in the downstream sand bed channel based on the magnitude of predicted bed elevations changes, but was very sensitive in the gravel bed reach.

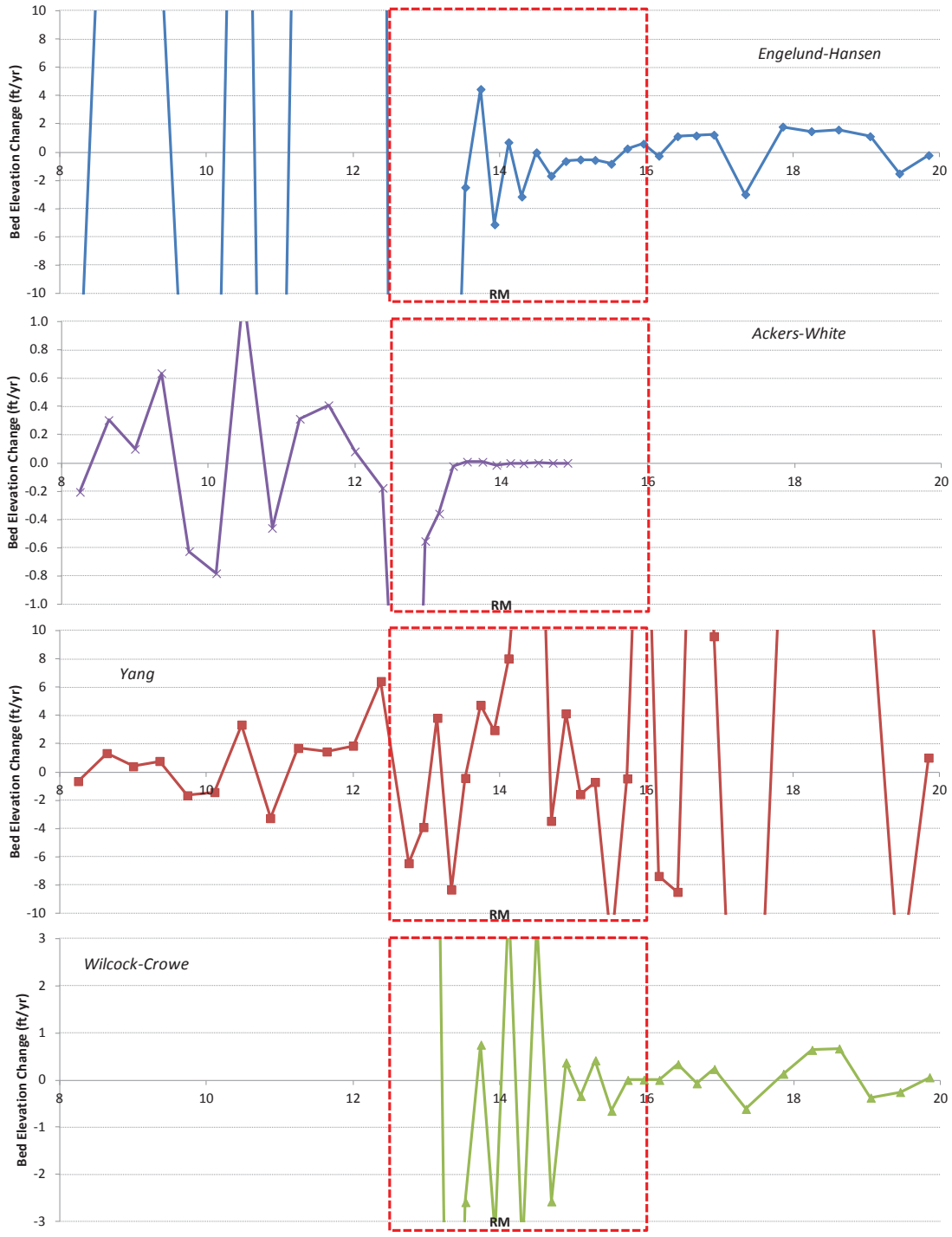

Figure 16. Comparison of predicted long term aggradation/degradation potential predicted by four sediment transport equations along the length of the Snohomish River above Ebey Slough. Shear stress was estimated using a uniform depth approximation. The red dashed box depicts the approximate extent of the gravel-sand transition zone.

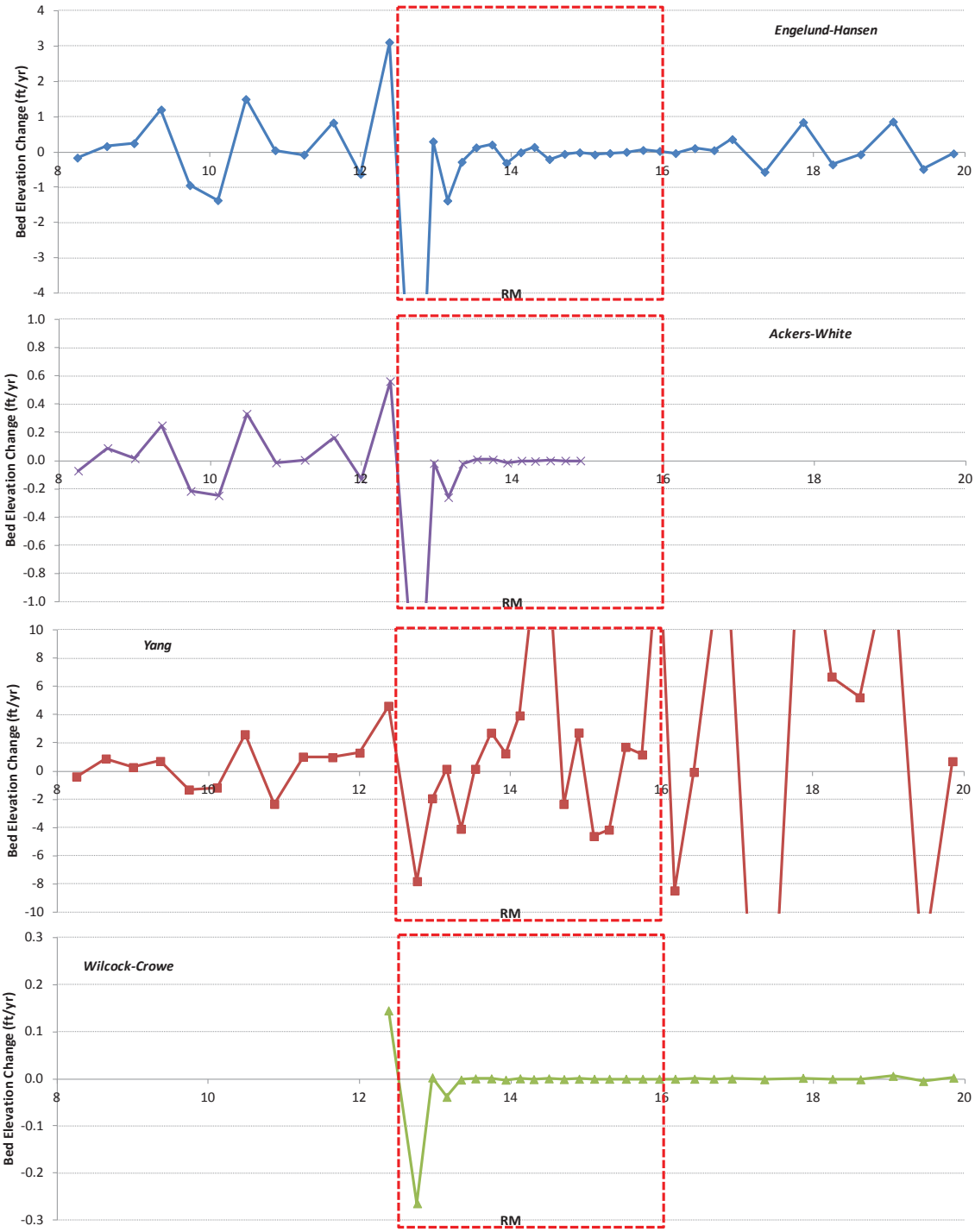

Figure 17. Comparison of predicted long term aggradation/degradation potential predicted by four sediment transport equations along the length of the Snohomish River above Ebey Slough. Shear stress was estimated using a roughness relation. The red dashed box depicts the approximate extent of the gravel-sand transition zone.

3.4 Channel Migration Patterns

Given the wide range in predicted magnitudes seen in Figures 16 and 17 depending on shear stress and transport rate equations used, we could not infer which of the predicted magnitudes of bed elevation change depicted in the graphs was most indicative of the likely actual level of change. Instead, however, we did observe consistent upstream-downstream trends in most analysis segments. In these cases, the classifications assigned following Table 7 were consistent across transport and shear stress equations, where the sign (+ or -) and relative differences in total transport volumes between successive cross-sections were preserved. In those cases, we concluded that analysis segments with consistent classifications (i.e., that were consistently predicted by all sediment transport equations to have similar relative aggradation/ degradation potential) were more likely to exhibit that tendency than not. Analysis segments with inconsistent classifications, where one transport equation predicted an aggradational tendency while another predicted a degradational tendency, were characterized as being subject to greater uncertainty.

In general, the equations collectively predicted similar trends in the direction of vertical stability (i.e., + or -) in most analysis segments in the sand bed and gravel bed reaches (Figures 16, 17; Plates 2, 3). However, trends were less consistent within the transition zone, which likely reflects a relatively abrupt reduction in grain size with distance downstream, and thus a transition in applicability of each sediment transport equation. Analysis segments with inconsistent predictions resulting from the uniform depth-shear stress estimator consisted of segments 6+7 (combined), 18, 19, 20, 24, 26, 29, 31, 35, and 38+39 (combined; Plate 2). There were fewer analysis segments with inconsistent predictions based on the roughness relation shear stress estimator, consisting of segments 10+11 (combined), 28, 31, 36, and 40+41 (combined; Plate 3). Results for the other segments were consistent in sign and often in the relative degree of instability; results for those segments were considered most reliable for use in locating project types (see Section 4). The inconsistent segments were evaluated more closely when identifying potential project types.

The aerial photograph series provided a relatively periodic determination of channel location, with intervening periods associated with at least one large flood event occurring that exceeded the 2-year event level (Figure 18). Despite numerous large flood events, the river has exhibited limited significant channel migration over the years. These results reflect diking and bank armoring that has occurred along nearly the entire length of the reach. Prior to the 1984 photographs, most activity occurred above the gravel-sand transition zone. After that, lateral instability was observed primarily in the vicinity of the mouth of the Pilchuck River in recent

years. Most historic channel migration activity occurred consistently in the vicinity of Thomas' Eddy (Figure 19), a short distance upstream of the gravel-sand transition zone. It could not be determined if the instability reflected gravel mining operations in Thomas' Eddy that ceased ca. 1991 (Collins 1995; R. Aldrich, Snohomish County, personal communication). There are no locations downstream of the gravel bed reach where natural channel migration processes can reconnect floodplain habitat or create new side channels presently. Forested islands have persisted in analysis segments 20 and 23-25 since 1933, with the area of the vegetated portions alternately growing and shrinking over time. This is approximately where the upstream hydraulic effects of tidal cycling are observed during low flow.

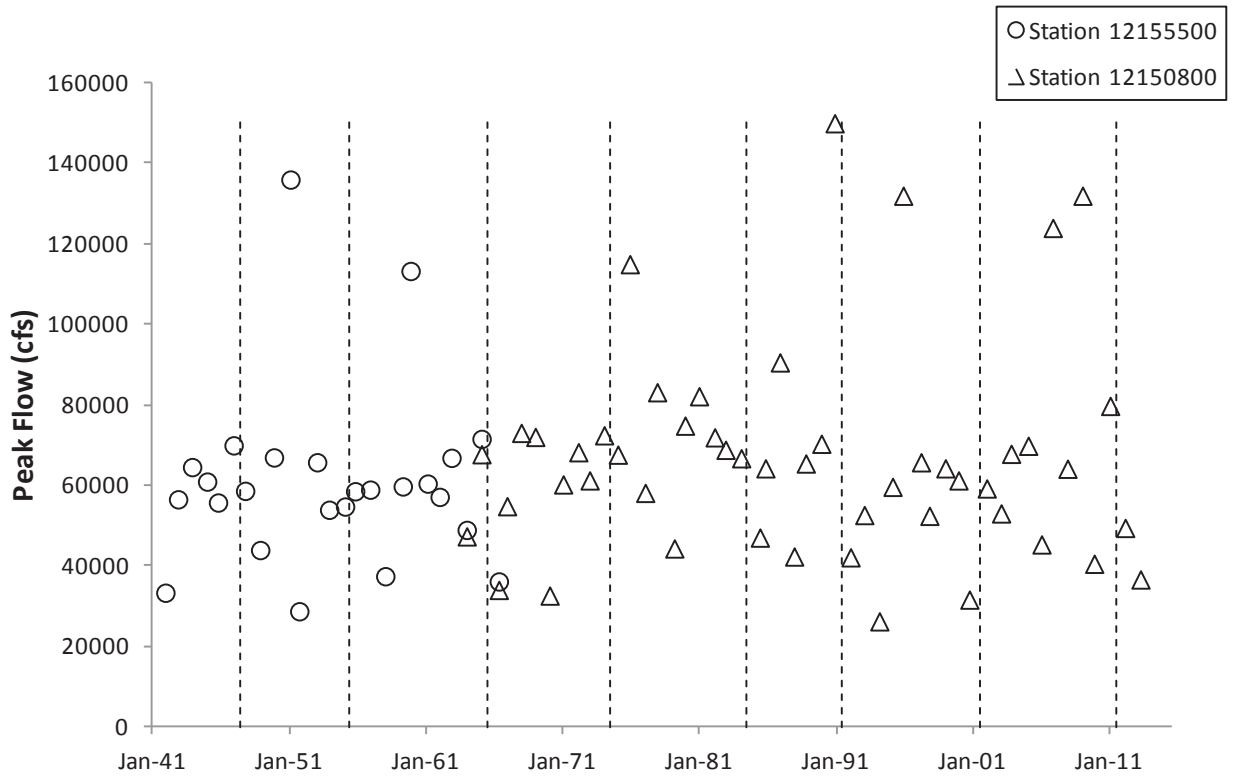

Figure 18. Annual peak flow time series encompassing the aerial photography date range, for the USGS gage in the Snohomish River near Monroe (#12150800) and at Snohomish (#12155500). Approximate times when each set of aerial photographs were taken are indicated by the dashed vertical lines.

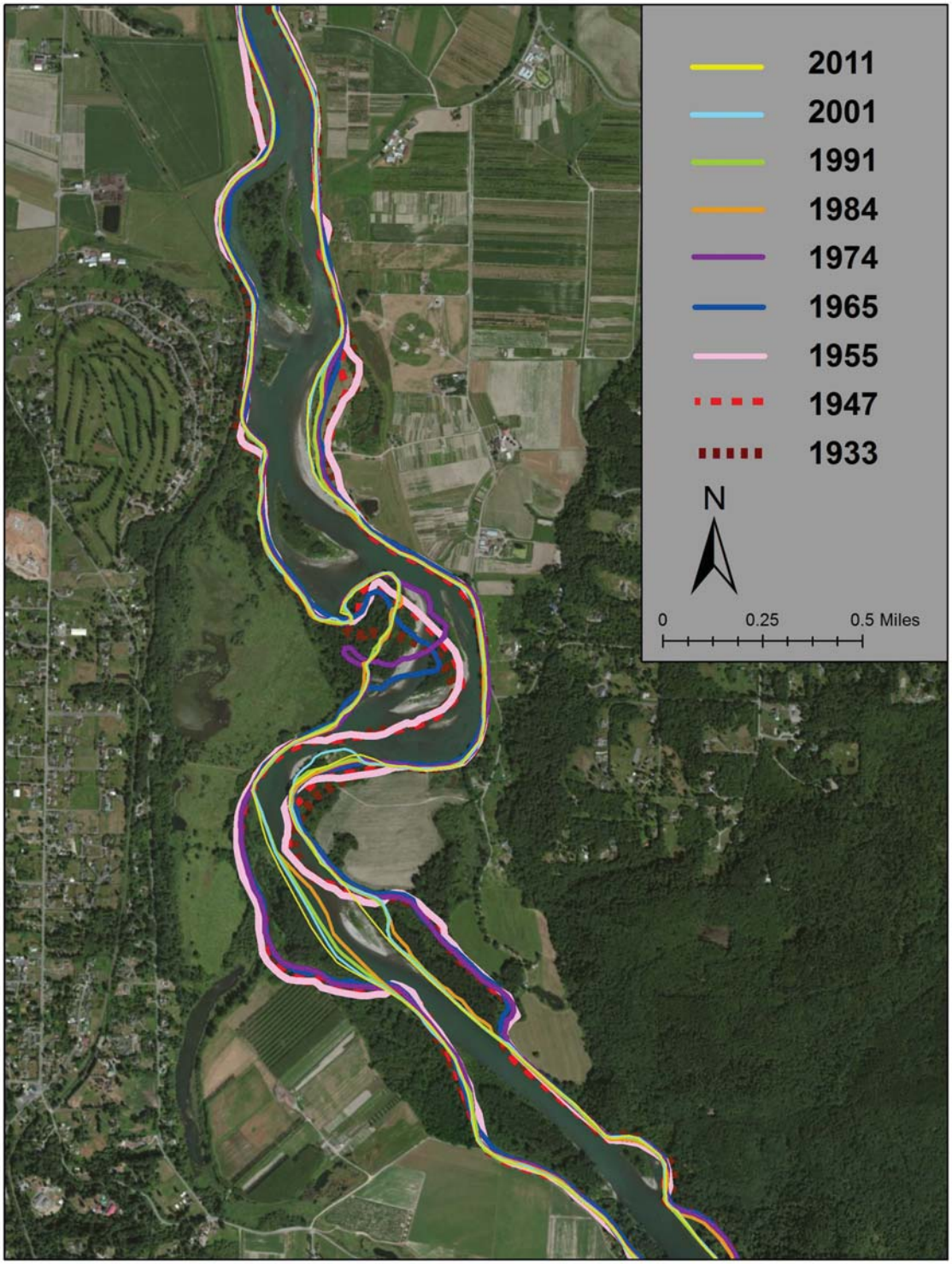

Figure 19. Historic changes in bankfull channel edge location in the vicinity of Thomas' Eddy, as inferred from the aerial photographic record.

3.5 Gravel/Sand Bar Storage Area Trends

Figure 20 presents cumulative plots of mapped active gravel/sand bar areas for selected years of aerial photography. The differences in cumulative area between curves at a given RM is suspected to reflect mostly tidal variation, error in interpreting older black and white aerial photographs, and, to some extent, the time passed between the previous large flood event and the date the photographs were taken (shorter time interval → greater amount of deposit surface area that has not become vegetated yet). Some general trends are evident nonetheless (Figure 20):

- The most active gravel/sand storage and reworking areas after 1947 have been located upstream of analysis segment 26, with greatest storage occurring in the vicinity of Thomas' Eddy and the upper segments of the gravel-sand transition zone.
- There was a substantial drop in active gravel/sand bar area that occurred between 1933 and 1947. After 1947, areas are within a general range that may be indicative of future variation. The cumulative areas appear to follow a cycling pattern, where active bar areas decreased over the 1947 to 1974 period, increased over the 1974 to 1991 period, and has been decreasing again since 1991. The two latter periods' increase and then decrease may reflect in large part the gravel harvesting that occurred in the vicinity of Thomas' Eddy between ca. 1962 and 1991 (Collins 1995).

Given that channel bank modifications and dikes have been generally in place since the 1947 aerial photographs, these results evident in Figure 20 indicate the possibility that active gravel/sand bar areas upstream of analysis segment 26 may be poised to increase again within the next 20-30 years.

3.6 Avulsion Risk

There are few floodplain channels in the assessment reach that are inundated at the 2-year flood level (Plate 4). Most of these channels are located in the vicinity of Thomas' Eddy. The joint avulsion risk ratings indicate that most of the channels that could be connected at the 2-year flood have a moderate rating of avulsion potential (Plate 5). There are isolated locations downstream where off-channel habitat connectivity opportunities exist, but these are generally proximal to infrastructure which could influence their overall feasibility for restoration. Those flow pathways that are crossed by paved roads (Plate 5) would have a lower risk of avulsion than others, however.

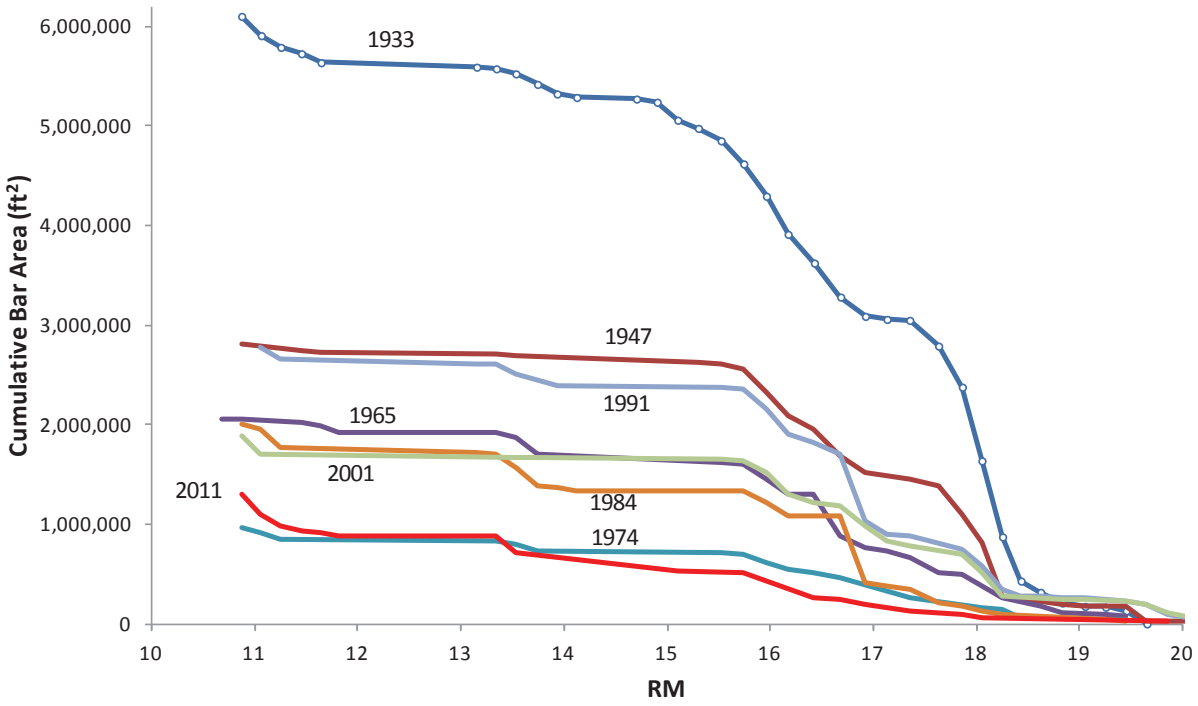

Figure 20. Cumulative area in the downstream direction of active, unvegetated gravel/sand bar surfaces in the main river channel visible and digitized from the historic aerial photography.

The individual and joint ratings represent relative risks amongst all potential flow paths based on physical characteristics known to affect the likelihood of avulsion. These risk ratings cannot be used to predict exactly where the channel will move during future storm events, but can be used to prioritize alternatives to reduce the risk of failure, or of potential impacts to property and infrastructure. The results depicted in Plates 4 and 5 are based on LiDAR data collected in 2006 and the 2D modeling. Specific ratings may change in the future depending on flooding and future channel erosion. It is not feasible to update the ratings each year after flooding because of the expense, however the ratings resulting from this analysis can still be used to assess general risk as described below, and provide an indication of relative differences in avulsion potential for possibly the next 10+ years.

4. SYNOPSIS OF ANALYSIS RESULTS AND IDENTIFICATION OF CONCEPTUAL RESTORATION PROJECTS

The following general patterns are indicated by the analysis results. The features indicated lead to river and fish habitat restoration projects that vary with characteristic river processes and erosion/deposition risks observed at the reach scale.

4.1 Summary of Large Scale Variation in Reach Geomorphic Characteristics

Three geomorphic reaches are roughly delineated by the assessment data and analysis results (Figure 21):

- Ebey Slough to RM ~12.5 (above the SR 9 bridge crossing):
  - Graded (i.e., ~ constant D_{50}) sand bed with relatively constant D_{50} all the way downstream to Ebey Slough;
  - Linear overall riverbed profile with lower gradient than upstream;
  - Generally consistent streamwise variation in aggradation/degradation potential irrespective of shear stress and sediment transport estimator;
  - No significant channel migration because of historic bank modifications; and
  - Most accessible floodplain flow paths are situated along the toe of dikes; few other floodplain flow paths evident behind dikes.
- RM ~12.5 to RM ~16.0 (near upstream ends of the French Creek and Marshland dike system):
  - Gravel-sand transition zone, fining rapidly in downstream direction;
  - Riverbed longitudinal profile has a relatively abrupt transition near the middle of the reach, with gradients above and below similar to gradients of gravel bed reach upstream and sand bed reach downstream;
  - Comparison of longitudinal profiles indicates the riverbed aggraded more in this reach than upstream or downstream since the late 1980s;
  - No significant channel migration because of historic bank modifications, with most activity limited to the mouth of the Pilchuck River and its gravel deposit.

- Lowest streamwise variation in aggradation/degradation potential near the upstream end, becoming more variable in the downstream direction, and tending to a larger degradation potential near the downstream end of the reach where the bed material is finest in size;
- Limited bar reworking activity, mostly limited to Pilchuck River deposits at the confluence;
- Floodplain channels consist of primarily abandoned oxbows; limited floodplain swales present within the bounds of diked margins.

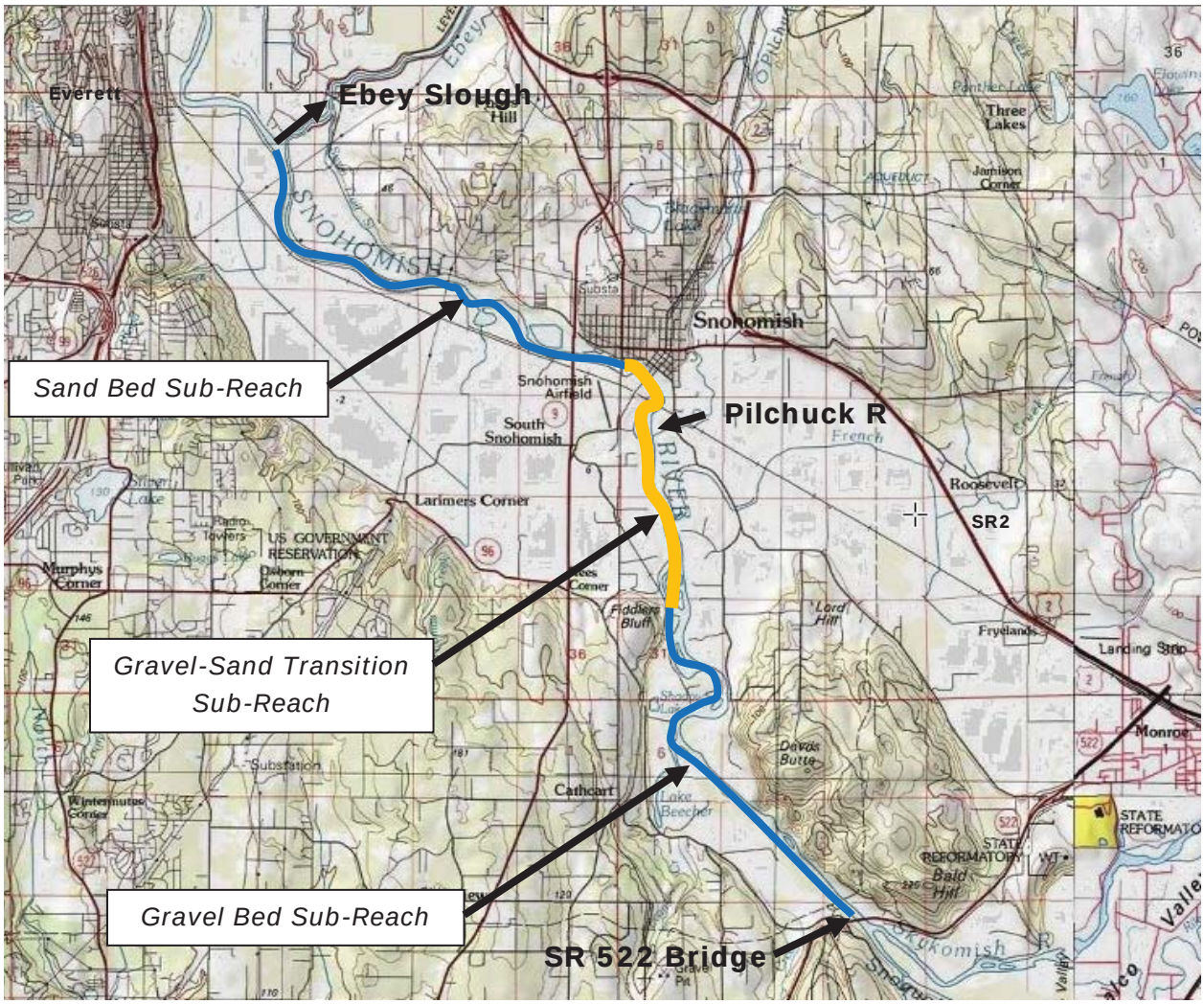

Figure 21. Locations of the three Snohomish River geomorphic sub-reaches defined by the assessment results.

- RM ~16.0 to SR 522:
  - Graded gravel bed channel with relatively constant D50;
  - Linear overall riverbed profile with similar gradient to upper portion of transition reach;
  - Channel migration observed in the vicinity of Thomas' Eddy but mostly prior to the 1984 photographs;
  - Some forested islands in lower portion of reach have expanded and contracted, but have generally persisted overall in the same locations over the aerial photographic record
  - Generally consistent streamwise variation in aggradation/degradation potential irrespective of shear stress and sediment transport estimator;
  - Most extensive reworking of gravel bars occurs in this reach; and
  - There are numerous floodplain channels that can be engaged at frequent flood flows.

4.2 Potential Restoration Projects

Two general types of restoration projects were identified along with the locations where they would be consistent with natural processes, subject to the following two caveats that must be considered when evaluating and selecting specific actions:

1. The projects are matched with existing river processes and watershed conditions, not future potential or pristine processes and conditions. It is the current geomorphic processes and conditions that will affect project performance and function over a reasonable project lifespan, which may be on the order of 10-20 years. Restoring watershed processes is generally beyond the scope of specific projects, and requires instead societal and institutional changes. At the same time, however, the projects identified below do have the potential to partially restore certain elements of natural watershed processes at the site and sub-reach scales. Channel migration and side channel connectivity projects have the greatest potential to restore natural river migration and floodplain connectivity processes, including cases where bank armoring is removed as part of the project. Erosion control and instream habitat structure projects will most directly improve instream habitat conditions.

2. The feasibility of each potential project also depends on consistency with economic and social aspects of land use, and with infrastructure constraints. For example, a project reconnecting one or more floodplain channels presently located behind dikes cannot be designed until the concept has been thoroughly vetted with stakeholders.

Riparian restoration (re-vegetation) projects are not identified, in large part because the conventional wisdom is that riparian restoration is recommended wherever possible. Such projects tend to reflect opportunities based more on land use patterns and willing land owners than on riverine geomorphic processes and conditions. In addition, riparian restoration can be integrated into each of the various project types below on a case-by-case basis.

Plate 6 depicts the locations of specific potential projects, which are identified in the following by the number depicted, along with the respective analysis segments involved. In addition, the general geomorphic characteristics promoting project success are identified for each type of project based on the results of the assessment. Other previously identified projects are also discussed in the context of the assessment results.

4.2.1 Floodplain and Side Channel Connectivity Projects

Connectivity projects could be planned and designed to function towards ensuring juvenile salmonid side channel habitat maintenance or restoration. Suitable sites would be located where there are large upstream-downstream sediment transport rate imbalances and a strong aggradation tendency such that a structure could be constructed to facilitate local deposition and set up conditions favoring channel migration away from the deposition location. In addition, there should be a relatively high avulsion risk at select locations deemed feasible according to land ownership, and bank armoring should be absent or can be removed or modified consistent with landowner goals. However, the extensive bank armoring protecting agricultural lands in the study reach constrains opportunities presently, with six locations potentially having reach scale conditions favoring functional structures that could lead to directing flow into former channel locations, backwater areas, and/or floodplain swales:

- Projects 1 & 2 (Segments 10-11):
    - Two potential re-connection points on the left bank, with instream roughness placed downstream of the inlets to backwater flood levels locally, and connection to the downstream end of Lake Beecher (note: a more detailed assessment of this latter connection should be performed regarding the potential for enhancing habitat suitability and accessibility by non-native smallmouth bass and other predators, and the associated risks to juvenile salmonids).

  - The Crabb dike on the right bank could be breached at one or two locations, with instream roughness structures installed strategically in the main channel in segment 11 to raise floodwaters locally for increased through-flow at the breach location(s). Creating only a backwater connection at the downstream end in lieu of breaching would be expected to have only short term benefits until deposition occurs and closes off the connection again, because the adjoining analysis segments are associated with a strongly aggradational tendency.

- Project 3 (Segments 14-15):
  - Beck dike candidate breach location on left bank, with instream roughness placed on exposed mid-channel gravel bars in segment 17 to raise upstream flood levels locally. Note that the avulsion risk is relatively high here, such that a project has the potential to lead to development of a major side channel through here over time. This project would impact public access to parts of the Bob Heirman Wildlife Park.
- Project 4 (Segment 18):
  - Frequently inundated, potential avulsion shortcut bypassing Thomas' Eddy that would become connected and possibly enlarge with instream roughness placed in segment 17 to raise upstream flood levels locally and increase connectivity during small, frequent floods.
- Project 5 (Segment 20):
  - Floodplain channel on right bank located on riverside of the French Slough Flood Control District dike, with instream roughness structures installed in one or both channel splits in segment 21 to increase connectivity during small, frequent floods. Flow pathway crosses a series of large ponds and an unpaved access road. Although islands in this vicinity tend to remain stable such that a flow split is more likely to remain stable here than upstream, project might still require some countermeasures to protect dike toe from erosion if channel enlarged substantially in future.
- Project 6 (Segment 40):
  - Off-channel habitat potentially available on right bank, flows under access road to Snohomish wastewater treatment facility. Low likelihood of avulsion through here, but may require additional flood protection of facility and access road. Long term trend for aggradation downstream of inlet location favors connectivity.

Placement of in-channel roughness to increase backwater not recommended from flood-protection perspective. Backwater habitat project not recommended because of local aggradation tendency in river favoring siltation.

- Project 7 (Segment 46):
    - Off-channel habitat connectivity project on left bank to open flow-through into Mud Bay, which is currently a backwater habitat. Segment is associated with moderate degradation tendency where likelihood of an inlet staying open is higher.

With the exception of Segment 46, these are locations where aggradational tendencies exist downstream of the proposed inlet location, and the target channels would be engaged more frequently at relatively low flood levels (below the 2 year event). In segment 46, the sediment transport analysis indicates the inlet is associated with a degradational tendency that might help enlarge the inlet or at minimum maintain it for the foreseeable future.

4.2.2 Instream Habitat Complexity Projects

The 2005 Salmon Conservation Plan indicates the need for river margin habitat complexity for juvenile and adult salmonids, and this application appears to be the most suitable for the study reach. Structures providing cover should be located in geomorphically inactive segments where sediment transport rate imbalances are minor, with negligible erosion or deposition tendency. In addition, avulsion potential should be relatively low where private property concerns exist. Straight reaches are best from a floater or boater safety concern, such that structures would be visible and flow patterns would not be directed at them, or alternatively, smaller structures should be placed below the low flow water level. Accordingly, the geomorphic analysis results are interpreted to suggest the following suitable locations:

- Project 8 (Segments 4-5):
    - A moderate degradation tendency in terms of vertical bed stability precludes recommending bank-attached structures, but ballasted logs sitting near the bank on the gravel riverbed may remain unburied.
- Project 9 (Segment 19):
    - A moderate degradation to possibly equilibrium tendency in terms of vertical bed stability precludes recommending bank-attached structures, but ballasted logs sitting on gravel riverbed may remain unburied.

- Project 10 (Segment 22):
  - An equilibrium tendency in terms of vertical bed stability implies a low likelihood of a bank-attached structure failing, but this is also a good place for instream ballasted structures.
- Projects 11-13 (Segments 23-25):
  - A moderate degradation to possibly equilibrium tendency in terms of vertical bed stability precludes recommending bank-attached structures, but ballasted logs sitting on gravel riverbed may remain unburied.
- Project 14 (Segment 31):
  - A moderate degradation to possibly equilibrium tendency in terms of vertical bed stability precludes recommending bank-attached structures, but ballasted logs sitting on gravel-sand bed may remain unburied.
- Project 15 (Segment 35):
  - An equilibrium to possibly mild degradation tendency in terms of vertical stability indicates a lower likelihood of a bank-attached structure failing, although design should factor in risk of undermining; also a good place for instream ballasted structures. Design will need to consider impacts to proposed WDFW boat launch site.
- Projects 16-18 (Segments 46-47, 50-53, 60-61):
  - A moderate degradation tendency in terms of vertical bed stability precludes recommending bank-attached structures, but ballasted logs sitting on sand bed may remain unburied.

4.2.3 Projects Identified Through Other Forums

Two potential projects have been identified previously in the course of discussions between Snohomish County and the French Slough Flood Control District related to erosion at the mouth of the Pilchuck River and evaluating options for upgrading pumping and drainage facilities and operations at the French Creek Pump Station. The results of the assessment may be useful for assessing each project's overall feasibility and design needs as controlled by reach scale geomorphic constraints, as follows:

- The sediment trapping efficiency results in Plates 2 and 3 and Figures 16 and 17 indicate that the long term tendency for bed elevation change in the Snohomish River is

somewhere between neutral to strongly degradational downstream of the confluence with the Pilchuck River depending on the shear stress and sediment transport equation used, and mildly to moderately aggradational upstream. At the same time, Figure 12 indicates that the Snohomish River has been generally aggrading overall in the vicinity of the confluence, and Plates 4 and 5 indicate the presence of potential avulsion pathways on the right bank floodplain that could affect a proposed WDFW/City of Snohomish boat launch facility. The bed elevation increase has likely influenced bedload transport in the Pilchuck River, where the increase base level is controlling grade upstream, reducing transport capacity to the mouth. Any project designed to address erosion problems at the confluence will need to consider these processes.

- With respect to the Pump Station location, the sediment transport results are more uncertain depending on the shear stress and sediment transport equation used. This outcome of the assessment likely reflects the location of the facility being near the upstream end of the gravel-sand transition zone. Where transport and deposition patterns are relatively complex. Changes to flood conveyance in the vicinity of the location will likely influence local depositional patterns substantially. If more detailed hydrodynamic modeling is performed, the linkage to sediment transport and resulting changes to channel and floodplain morphology will need to be assessed carefully.

4.3 Level of Confidence in Analysis and Results

The longitudinal profiles and/or variation of channel gradient, thalweg elevation, grain size, sediment transport analysis predictions of aggradation/degradation potential, channel migration rates, and size and extent of side channel changes over time, all consistently point to the four geomorphic sub-reaches outlined above. More site specific analysis and design will be required to evaluate specific projects and management actions, but the results presented here provide a quantitative estimate of reach scale hydraulic and erosion processes that will affect general suitability of specific measures. The information can be used to infer relative risk associated with different restoration activities (e.g., channel and floodplain connectivity, instream/bank stabilization structures, channel migration training, and bank revetment removal), with respect to whether projects would work against or with natural sedimentation and channel forming processes.

The level of uncertainty about each individual analysis varies depending on the type of data, and can be inferred in many cases from the scatter of data depicted in the graphs above. Specific cases are identified below:

- The flood level and sediment transport predictions should not be used to predict duration of floodplain inundation. Limited field surveyed flood level data were used to calibrate the 2D hydrodynamic model, and drainage rate information was not available at this time for areas located behind major floodgate and pump station facilities.
- Typical sediment transport rate prediction errors range within an order of magnitude. However, the relative differences in sediment transport potential predicted for successive transects should be preserved and not meaningfully affect the results presented in this report, or erosion risk determinations based on those results.
- The channel migration traces are generally accurate for the main channel and major side channels. Smaller side channels not visible in the aerial photographs were delineated as part of the avulsion risk analysis using the LiDAR data. The collective digitized channel traces for the present and avulsion risk analyses should provide for a reasonable delineation of the channel migration zone, although GLO survey maps could also be digitized to evaluate longer term historic stability if needed.

5. REFERENCES

Ackers, P., and W.R. White. 1973. Sediment transport: new approach and analysis. ASCE Journal of the Hydraulics Division, 99(11):2041-2060.

Church, M.A., D.G. McLean, and J.F. Wolcott. 1987. River bed gravels: Sampling and analysis. Ch. 3 in: Thorne, C.R., J.C. Bathurst, and R.D. Hey [Eds.]. Sediment transport in gravel-bed rivers. John Wiley and Sons, New York, NY. 995 p.

Collins, B. 1995. Riverine Gravel Mining in Washington State, Physical Effects with Implications for Salmonid Habitat, and Summary of Government Regulations. United States Environmental Protection Agency. Seattle, WA.

DeVries, P. 2000. Scour in Low Gradient Gravel Bed Streams: Patterns, Processes, and Implications for the Survival of Salmonid Embryos. Ph.D. dissertation, University of Washington, Seattle, Washington.

Engelund, F. and E. Hansen. 1967. A monograph on sediment transport in alluvial streams. Teknisk Forlag, Copenhagen, Denmark, 65 p.

King, I. 2011. User's Guide to RMA2, v4.5. U.S. Army, Engineering and Development Center, Waterways Experiment Station, Coastal and Hydraulic Laboratory.

Kondolf, G.M. 2000. Some Suggested Guidelines for Geomorphic Aspects of Anadromous Salmonid Habitat Restoration Proposals. Restoration Ecology 8(1): 48-56.

Kondolf, G.M., M.W. Smeltzer, and S.F. Railsback. 2001. Design and Performance of a Channel Reconstruction Project in a Coastal California Gravel-Bed Stream. Environmental Management 28(6): 761-776.

Miall, A.D. 1977. A Review of the Braided-river Depositional Environment. Earth-Science Reviews, Volume 13, Issue 1, May 1977, Pages 1-62, ISSN 0012-8252. DOI: 10.1016/0012-8252(77)90055-1.

Rapp, C.F., and T.B. Abbe. 2003. A Framework for Delineating Channel Migration Zones. Washington State Department of Ecology, Final Draft Publication #03-06-027. Olympia, Washington.

Richards, K. 1982. Rivers: Form and process in alluvial channels. Methuen, London. 361 p.

Schmidt, L.J., and J.P. Potyondy. 2004. Quantifying channel maintenance instream flows: an approach for gravel-bed streams in the Western United States. Gen. Tech. Rep. RMRS-GTR-128. Fort Collins, CO: U.S. Department of Agriculture, Forest Service, Rocky Mountain Research Station. 33 p.

Snohomish County Department of Public Works, Surface Water Management (SWM). 2003. Snohomish River Confluence Reach Analysis: Phase 1 feasibility study final report. http://www.snohomishcountywa.gov/ArchiveCenter/ViewFile/Item/2155. July.

Wilcock, P.R., and J.C. Crowe. 2003. Surface-based transport model for mixed-size sediment. Journal of Hydraulic Engineering, 129(2), 120-128.

Wissmar, R.C, and R.L. Beschta. 1998. Restoration and Management of Riparian Ecosystems: A Catchment Perspective. Freshwater Biology 40: 571-585.

Yang, C.T. 1973. Incipient motion and sediment transport. Journal of the Hydraulics Division, 99(10), 1679-1704.

APPENDIX A

Magnified Views of Boxed Areas Delineated in Figure 14 Showing Predicted Velocity Vectors at Higher Resolution

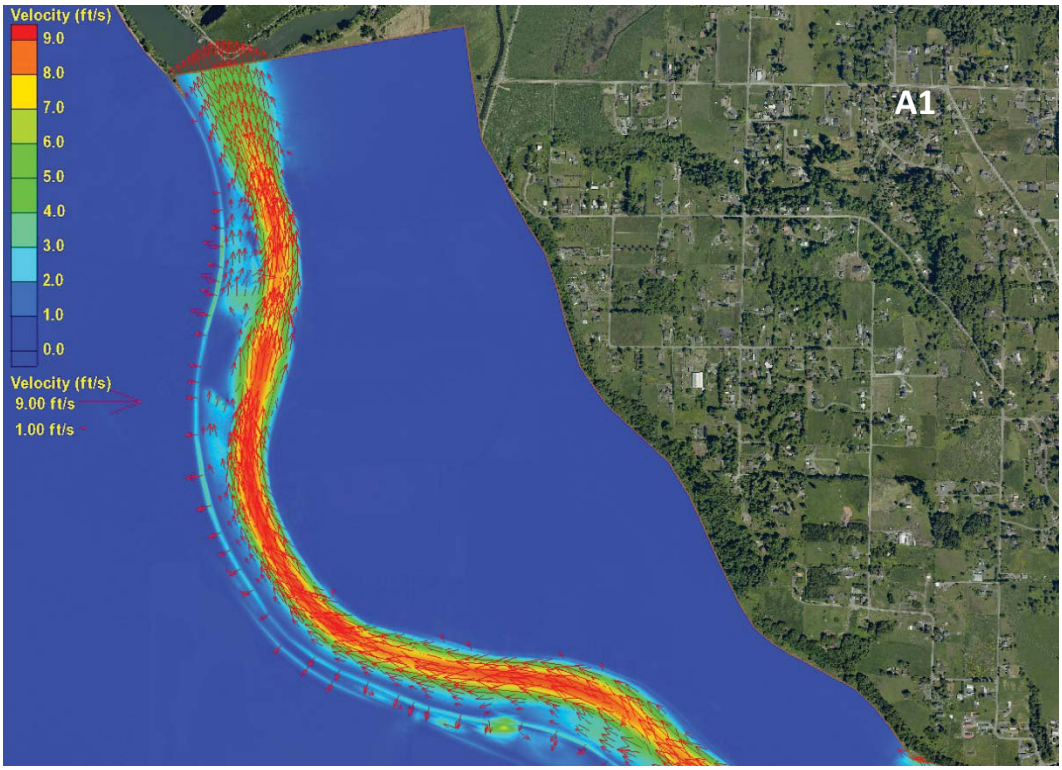
Velocity (ft/s)
9.0
8.0
7.0
6.0
5.0
4.0
3.0
2.0
1.0
0.0
Velocity (ft/s)
9.00 ft/s
1.00 ft/s
A1

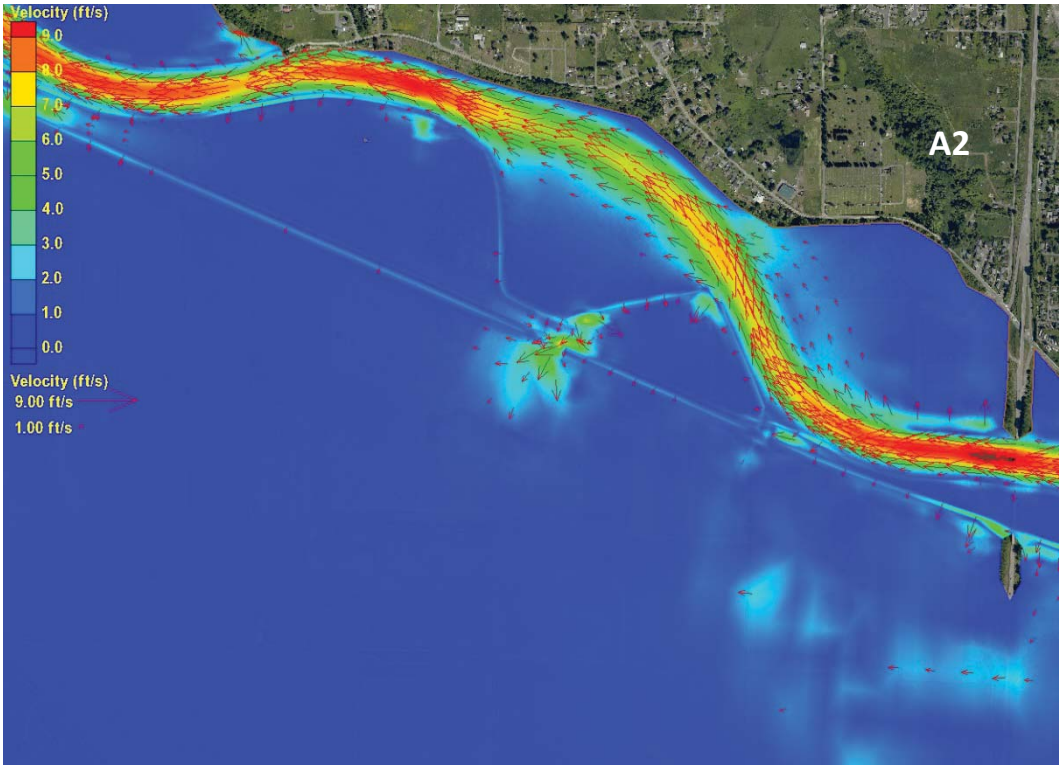
Velocity (ft/s)
9.0
8.0
7.0
6.0
5.0
4.0
3.0
2.0
1.0
0.0
Velocity (ft/s)
9.00 ft/s
1.00 ft/s
A2

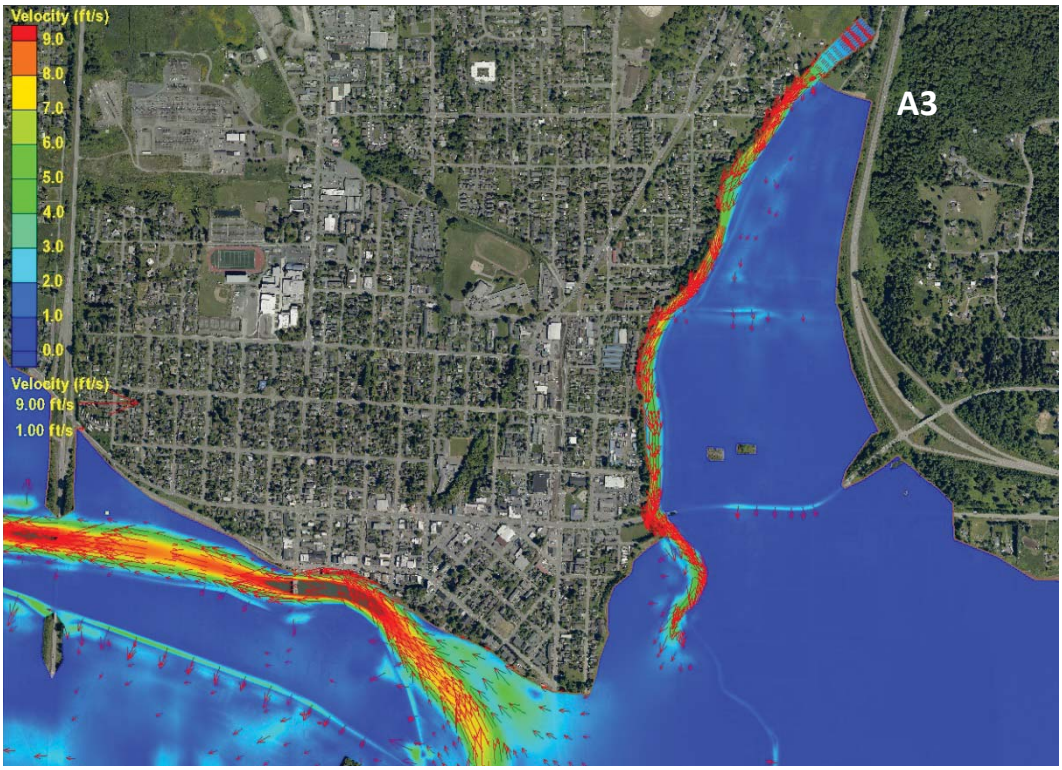
Velocity (ft/s)
9.0
8.0
7.0
6.0
5.0
4.0
3.0
2.0
1.0
0.0
Velocity (ft/s)
9.00 ft/s
1.00 ft/s
A3

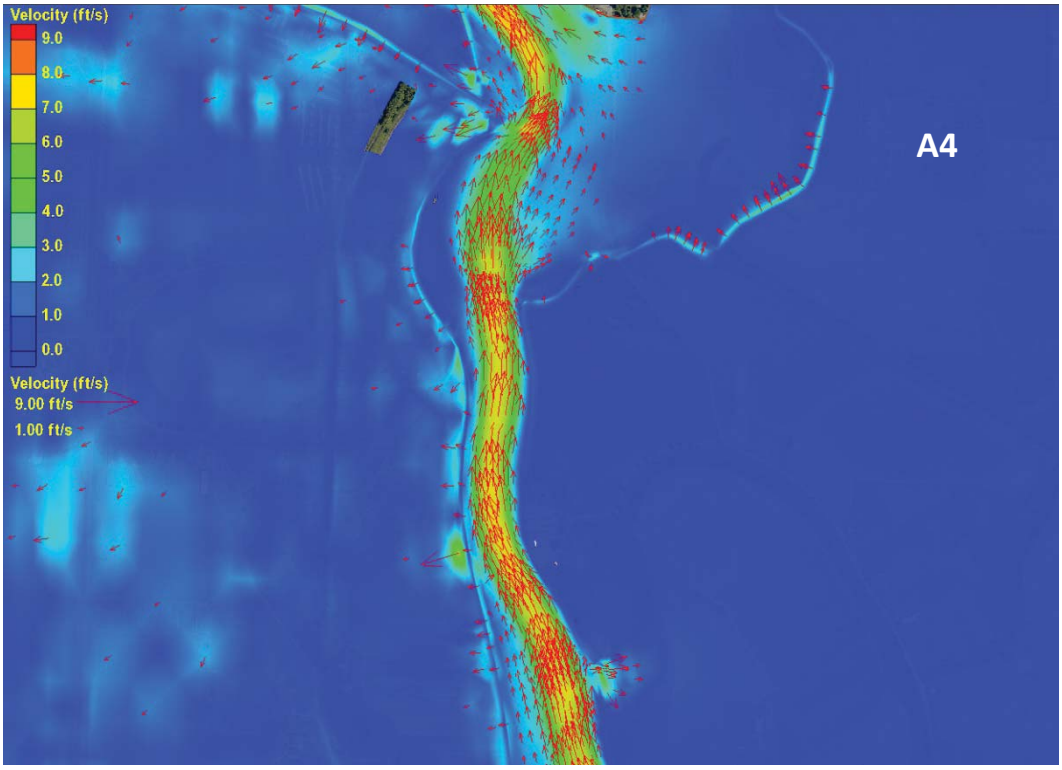
Velocity (ft/s)
9.0
8.0
7.0
6.0
5.0
4.0
3.0
2.0
1.0
0.0
Velocity (ft/s)
9.00 ft/s
1.00 ft/s
A4

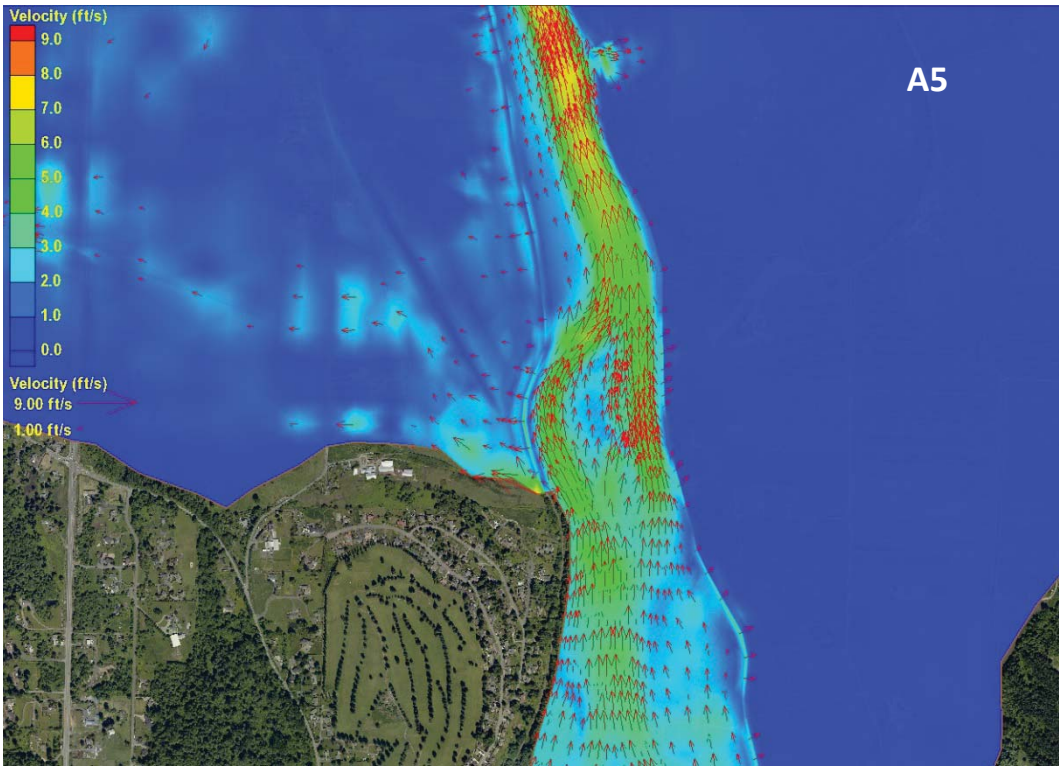
Velocity (ft/s)
9.0
8.0
7.0
6.0
5.0
4.0
3.0
2.0
1.0
0.0
Velocity (ft/s)
9.00 ft/s
1.00 ft/s
A5

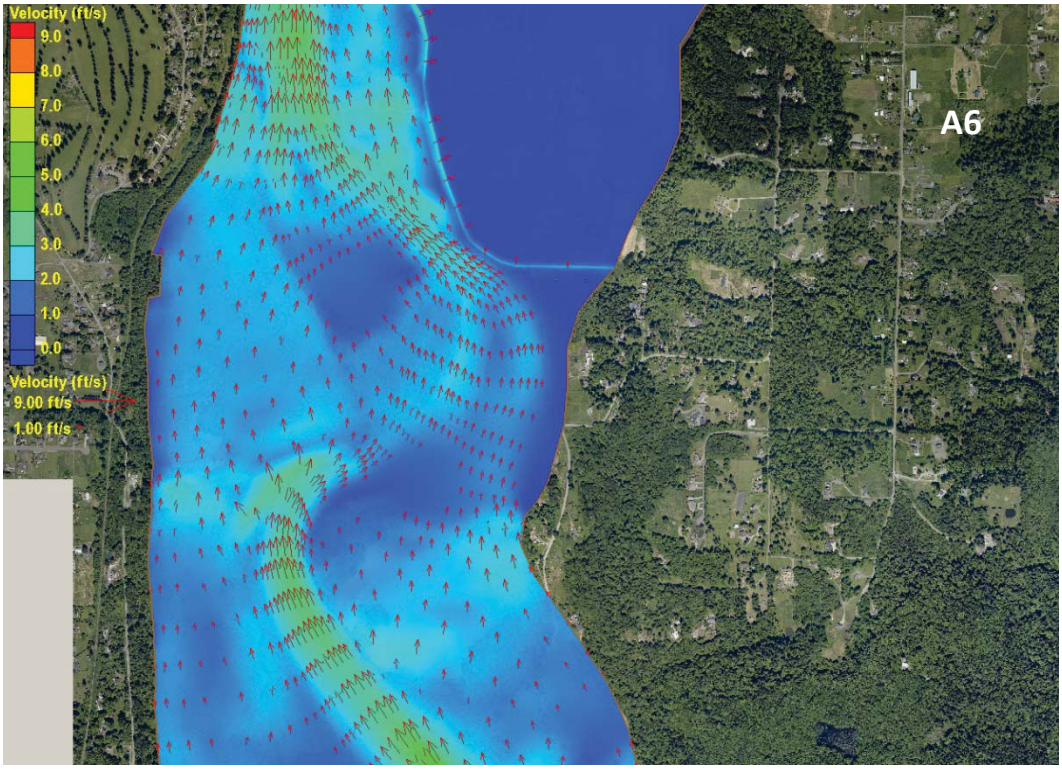
Velocity (ft/s)
9.0
8.0
7.0
6.0
5.0
4.0
3.0
2.0
1.0
0.0
Velocity (ft/s)
9.00 ft/s
1.00 ft/s
A6

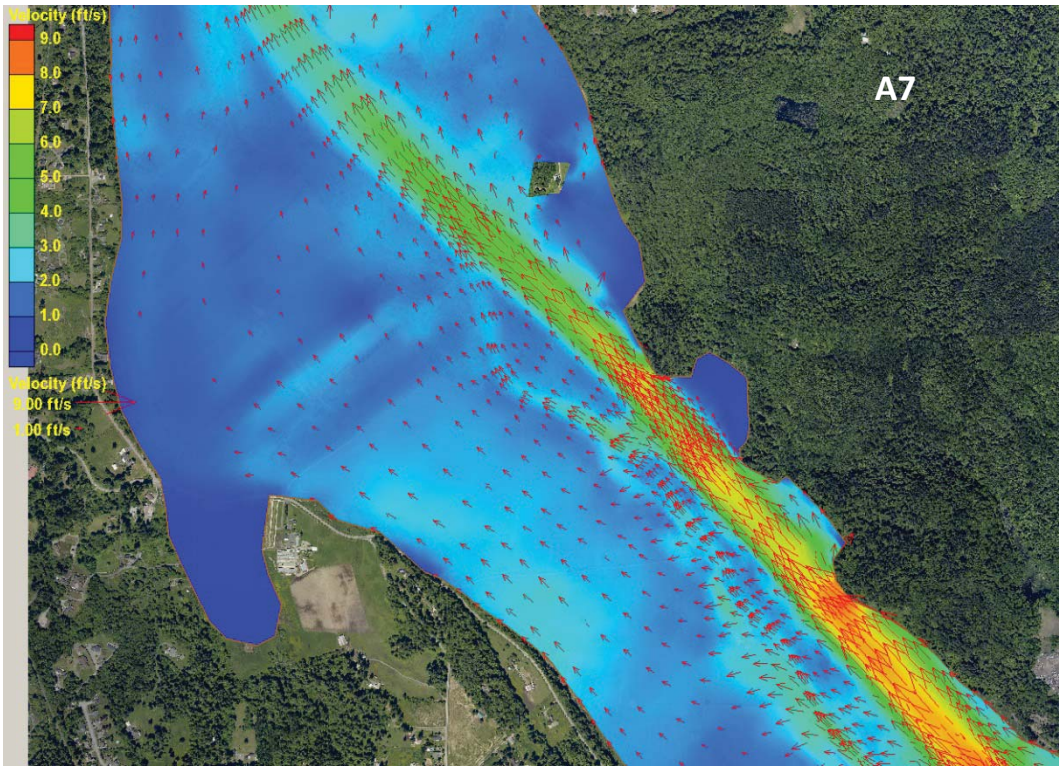
Velocity (ft/s)
9.0
8.0
7.0
6.0
5.0
4.0
3.0
2.0
1.0
0.0
Velocity (ft/s)
9.00 ft/s
1.00 ft/s
A7

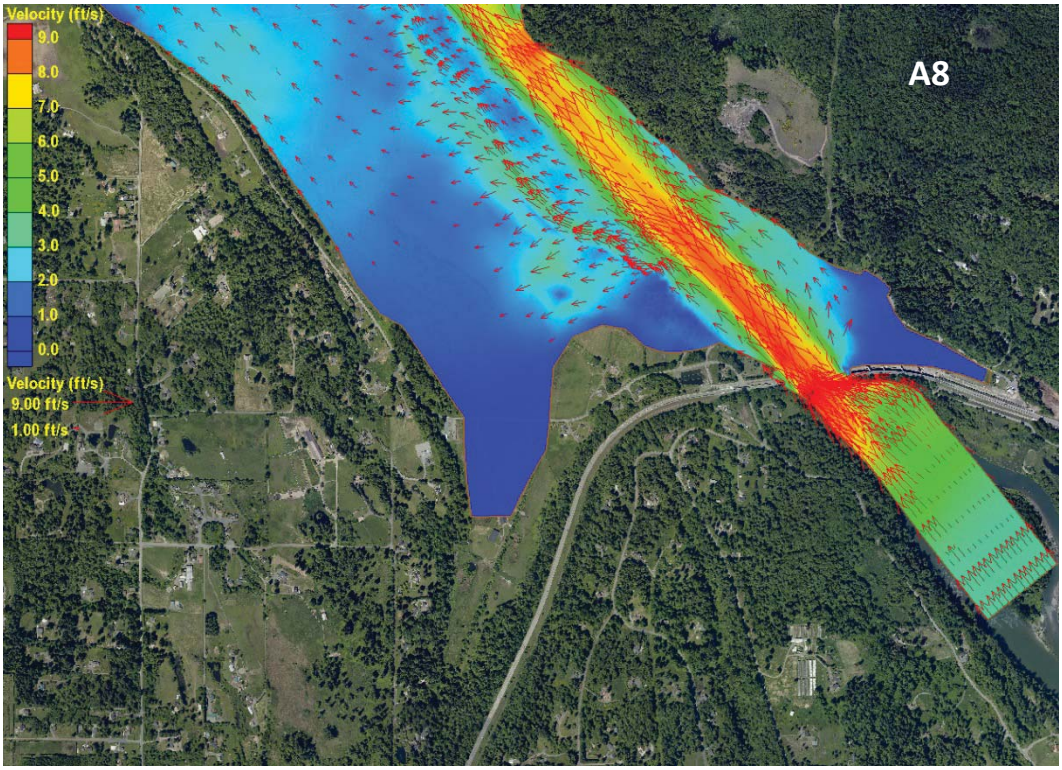
Velocity (ft/s)
9.0
8.0
7.0
6.0
5.0
4.0
3.0
2.0
1.0
0.0
Velocity (ft/s)
9.00 ft/s
1.00 ft/s
A8

APPENDIX B

Plates

List of Plates

Plate 1. Location of analysis segments established to evaluate and present GIS data for the Snohomish River geomorphic reach analysis.

Plate 2. Spatial variation in erosional and depositional trends in the Snohomish River analysis reach as suggested by sediment transport modeling using four different sediment transport equations with shear stress predicted by the uniform flow approximation; classifications are as defined in Table 7 and are averages of ratings defined for each of the transport equations. Lateral extent depicted is based on the extent of channel confinement imposed by dikes.

Plate 3. Spatial variation in erosional and depositional trends in the Snohomish River analysis reach as suggested by sediment transport modeling using four different sediment transport equations with shear stress predicted by a roughness relation; classifications are as defined in Table 7 and are averages of ratings defined for each of the transport equations. Lateral extent depicted is based on the extent of channel confinement imposed by dikes.

Plate 4. Flood engagement level ratings of potential avulsion pathways characterized according to lowest of three flood levels (2-, 10- and 100-year recurrence intervals) at which floodplain or off-channel flow may occur. Tracings and ratings were based on 2006 topography.

Plate 5. Joint avulsion potential ratings of potential avulsion pathways characterized according to weighted sums of flood flow level, longitudinal gradient, and floodplain soil K_w erodibility factor ratings. Segments that cross paved roads (i.e., reduced avulsion risk) are also indicated. Tracings and ratings were based on 2006 topography.

Plate 6. Potential general locations of different types of restoration projects identified in this assessment that address Snohomish River Basin Salmon Conservation Plan goals and that are consistent with natural processes in the Snohomish River.